

Therapeutic Effect of Human Adipose Tissue-Derived Mesenchymal Stem Cells in Experimental Corneal Failure Due to Limbal Stem Cell Niche Damage

SARA GALINDO  ^{a,b} JOSÉ M. HERRERAS, ^{a,b} MARINA LÓPEZ-PANIAGUA, ^{a,b} ESTHER REY, ^{a,b}
ANA DE LA MATA, ^{a,b} MARÍA PLATA-CORDERO, ^{a,b} MARGARITA CALONGE, ^{a,b} TERESA NIETO-MIGUEL ^{a,b}

Key Words. Adipose tissue-derived mesenchymal stem cells • Limbal stem cell deficiency • Corneal failure • Ocular surface failure • Mesenchymal stem cell transplantation • In vivo experimental eye models

^aInstitute of Applied Ophthalmobiology (IOBA), University of Valladolid, Valladolid, Spain; ^bCIBER-BBN (Biomedical Research Networking Center in Bioengineering, Biomaterials and Nanomedicine), Carlos III National Institute of Health, Spain

Correspondence: Teresa Nieto-Miguel, Institute of Applied Ophthalmobiology (IOBA), Universidad de Valladolid, Campus Miguel Delibes, Paseo de Belén 17, E-47011, Valladolid, Spain. Telephone: 34-983-184750; Fax: 34-983-184762; e-mail: tnieto@ioba.med.uva.es; or Sara Galindo, Institute of Applied Ophthalmobiology (IOBA), Universidad de Valladolid, Campus Miguel Delibes, Paseo de Belén 17, E-47011, Valladolid, Spain. Telephone: 34-983-184750; Fax: 34-983-184762; e-mail: sgalindor@ioba.med.uva.es

Received November 28, 2016; accepted for publication June 17, 2017; first published online in *STEM CELLS EXPRESS* July 31, 2017.

[http://dx.doi.org/
10.1002/stem.2672](http://dx.doi.org/10.1002/stem.2672)

ABSTRACT

Limbal stem cells are responsible for the continuous renewal of the corneal epithelium. The destruction or dysfunction of these stem cells or their niche induces limbal stem cell deficiency (LSCD) leading to visual loss, chronic pain, and inflammation of the ocular surface. To restore the ocular surface in cases of bilateral LSCD, an extraocular source of stem cells is needed to avoid dependence on allogeneic limbal stem cells that are difficult to obtain, isolate, and culture. The aim of this work was to test the tolerance and the efficacy of human adipose tissue-derived mesenchymal stem cells (hAT-MSCs) to regenerate the ocular surface in two experimental models of LSCD that closely resemble different severity grades of the human pathology. hAT-MSCs transplanted to the ocular surface of the partial and total LSCD models developed in rabbits were well tolerated, migrated to inflamed tissues, reduced inflammation, and restrained the evolution of corneal neovascularization and corneal opacity. The expression profile of the corneal epithelial cell markers CK3 and E-cadherin, and the limbal epithelial cell markers CK15 and p63 was lost in the LSCD models, but was partially recovered after hAT-MSC transplantation. For the first time, we demonstrated that hAT-MSCs improve corneal and limbal epithelial phenotypes in animal LSCD models. These results support the potential use of hAT-MSCs as a novel treatment of ocular surface failure due to LSCD. hAT-MSCs represent an available, non-immunogenic source of stem cells that may provide therapeutic benefits in addition to reduce health care expenses. *STEM CELLS* 2017;35:2160–2174

SIGNIFICANCE STATEMENT

Partial and total ocular limbal stem cell deficiency (LSCD) models in rabbits emulate, respectively, mild and moderate-to-severe LSCD in humans. Herein, we show that human adipose tissue-derived mesenchymal stem cells (hAT-MSCs) transplanted to the ocular surface of LSCD rabbit eyes were well-tolerated, migrated to inflamed tissues, reduced inflammation, and restrained the evolution of corneal neovascularization and opacity. Additionally, the hAT-MSCs partially restored the corneal and limbal epithelial phenotypes. Thus, hAT-MSCs, which are readily available and non-immunogenic, represent a potential novel therapy for human ocular surface failure due to loss of functional limbal stem cells.

INTRODUCTION

The integrity of the corneal epithelium plays a critical role in maintaining transparency and visual function. Limbal stem cells, located in the basal epithelium of the corneoscleral limbus, are responsible for the continuous renewal of the corneal epithelium [1–3]. Destruction or dysfunction of limbal stem cells or their niche induces limbal stem cell deficiency (LSCD),

which can be triggered by a multitude of conditions such as chemical or thermal burns, cicatrizing-autoimmune pathologies, infections, and so on. LSCD is characterized by the invasion of conjunctival epithelium onto the cornea, transforming it into an opaque, vascularized, and defective epithelium. This usually results in chronic pain, persistent ocular surface inflammation, and corneal blindness [4, 5].

The treatment of choice for unilateral cases of LSCD is cultivated limbal epithelial transplantation (CLET) in which autologous limbal epithelial cells, including stem cells, are harvested from the contralateral healthy eye and cultured to expand the stem cell population before transplantation [6–8]. However, the high prevalence of bilateral cases makes allogeneic CLET, accompanied by essential immunosuppression, the treatment of choice despite the increased risk of patient morbidity and medical expenses [8]. Therefore, the use of an extraocular source of stem cells would be desirable to avoid dependence on allogeneic limbal stem cells, which are difficult to obtain, isolate, and culture and which can induce immune rejection.

In recent years, the use of mesenchymal stem cells (MSCs) has tremendously increased in cell therapy treatments [9–12] because they are relatively easy to obtain from a variety of tissue types, including bone marrow (BM), adipose tissue (AT), umbilical cord, etc. MSCs have the capacity to differentiate toward mesodermal and non-mesodermal cell lineages [13], and importantly, they also possess immunomodulatory and non-immunogenic properties [14], obviating the need for immunosuppression.

There is abundant evidence from both *in vitro* and *in vivo* studies regarding the potential use of BM-derived MSCs (BM-MSCs) for ocular surface regeneration. All published data have reported promising results in animal models and have demonstrated significant corneal regeneration, improved corneal transparency, and rapid healing associated with the restoration of vision [11, 15, 16]. AT is another source of MSCs (AT-MSCs) and is more accessible, and more cost-effective, and a safer source of MSCs than BM [17]. Recent studies have provided new insights about the beneficial role that AT-MSCs could have in corneal epithelial regeneration. Our research group and others have demonstrated that AT-MSCs express corneal epithelial markers under basic culture conditions, suggesting that these cells may have some inherent properties to regenerate the corneal epithelium [18, 19]. In experimental models of LSCD, administration of AT-MSCs subconjunctivally [20], topically [21–23], or overlaid on scleral contact lenses or nanofiber scaffolds [24, 25] promotes regeneration of the corneal epithelium. Additionally, a case report in which AT-MSCs were applied topically to a patient with persistent sterile epithelial defects supports the potential benefit of this modality [26].

The success or the failure of any new therapy clearly depends on the severity of the target pathology, and therefore, it is necessary to develop animal models that accurately resemble the different progressive grades of the human diseases. In this regard, we report here the development of two animal models of LSCD that resemble the human progressive grades of severity. With these models, we report not only the changes in the clinical signs before and after AT-MSC transplantation but also the expression profiles of corneal, limbal, and conjunctival molecular markers. The aim of this work was to test the tolerance and the efficacy of human AT-MSCs to regenerate the ocular surface in *in vivo* experimental models that closely resemble human LSCD pathology.

MATERIALS AND METHODS

This study was approved by the IOBA Research Committee and the Ethics and Animal Care Committees of the University of Valladolid. All procedures followed the guidelines of the Declaration of Helsinki for research involving human tissues

and the standards of Association for Research in Vision and Ophthalmology as provided in the Statement for the Use of Animals in Ophthalmic and Visual Research.

Isolation, Expansion, and Characterization of hAT-MSCs

Subcutaneous human AT was provided by a medical aesthetic clinic (Europa Clinic, Valladolid, Spain) after a liposuction procedure on a single subject who provided written informed consent. Cells were isolated using the procedure described by Zuk et al. [27]. The lipoaspirate was digested at 37°C for 30 minutes with 0.075% collagenase type I (Life Technologies, Inchinnan, UK, <http://www.lifetechnologies.com>), incubated with 160 mM NH₄Cl erythrocyte lysing buffer (Sigma-Aldrich, St. Louis, MO, <http://www.sigmaldrich.com>) and filtered through 100 µm and 40 µm mesh filters (BD Falcon, Franklin Lakes, NJ, <https://www.bdbiosciences.com>). Cells were cultured until passage 3–4, in low-glucose (1 g/L) Dulbecco's modified Eagle's medium (DMEM), GlutaMAX, 1 mM sodium pyruvate (Life Technologies), 10% fetal bovine serum (FBS) (Life Technologies), 100 U/mL penicillin, and 100 µg/mL streptomycin (Life Technologies) at 37°C, 5% CO₂, and 95% humidity. Cell passages were made at a density of 3,000–6,000 cells per square centimeter when cultures reached 90% of confluence. The cells were characterized as described previously [18] in accordance with the International Society for Cellular Therapy (ISCT) position statement [28].

hAT-MSC Culture on Amniotic Membranes

Before the seeding, P3–4 hAT-MSCs were labeled with 5'-bromo-2'-deoxyuridine (BrdU, BD Biosciences, San Jose, CA, <https://www.bdbiosciences.com>). hAT-MSCs at 70% confluence were incubated with 10 µM BrdU in culture medium (200 µL/cm²) for 24 hours at 37°C. Human amniotic membrane (AM) was obtained from cesarean section after written informed consent was obtained and provided by San Francisco Clinic (León, Spain). Each AM was processed using the procedure described previously by Tseng [29] with some modifications. The AMs were received in physiological saline solution containing antibiotics, cut into pieces of approximately 4 cm × 4 cm, and stored in DMEM with glycerol (Sigma-Aldrich) (1:2) at –80°C. Immediately before use, the AMs were thawed, washed with Hank's balanced salt solution (HBSS, Life Technologies) three times for 10 minutes, and treated with 0.25% trypsin–ethylenediaminetetraacetic acid (Life Technologies) for 10 minutes at room temperature. After that, the trypsin was inactivated with FBS, and the AMs were scraped to remove the epithelium and cut into 2 cm × 2 cm pieces. hAT-MSCs (2.5×10^5) were seeded onto the AM pieces in 250 µL of culture medium and allowed to adhere. After 2 hours, 200 µL/cm² of culture medium was added.

In Vivo Models of LSCD

The first LSCD model was created with a surgical 180° limbal peritomy (superior and temporal, $n = 15$) performed by crescent knife, removing 1–1.5 mm of the adjacent conjunctiva to ensure the total removal of the limbal niche. Hereinafter, this is referred to as the "partial LSCD." The second LSCD model was similarly created but with a 360° limbal peritomy ($n = 12$). It is referred to as the "total LSCD." Topical anti-inflammatory and antibiotics including two drops of Maxitrol (3,500 IU/mL neomycin, 6,000 IU/mL polymyxin B, and 1 mg/mL dexamethasone, Alcon, Barcelona, Spain, <https://wwwalcon.es>); 3 mg/g

tobramycin ointment (Tobrex, Alcon), systemic analgesia (0.02 mg/kg buprenorphine, Buprex, Indivior, Bristol, UK, <http://www.indivior.com>) and antibiotics (5 mg/kg enrofloxacin, Alsir, Esteve, Barcelona, Spain, <https://www.esteve.es>) were administered daily for 5 days.

The partial and total LSCD models were created in adult female New Zealand white rabbits (*Oryctolagus cuniculus*). The eyes were divided in five groups: Group 0, healthy eyes ($n = 6$); Group 1, partial LSCD without treatment ($n = 6$) in eyes that were contralateral to Group 0; Group 2, partial LSCD transplanted with AM without hAT-MSCs ($n = 3$); Group 3, partial LSCD transplanted with hAT-MSCs on AM ($n = 6$); Group 4, total LSCD without treatment ($n = 6$); and Group 5, total LSCD transplanted with hAT-MSCs on AM ($n = 5$) (Supporting Information Table S1). The rabbits were anesthetized by intramuscular injection of 50 mg/kg ketamine (Imalgene 1000, Merial, Lyon, France, <http://merial.com>) and 7 mg/kg xylazine (Rompun, Bayer, Leverkusen, Germany, <http://www.bayer.com>), complemented with topical ophthalmic anesthesia (1 mg/mL tetracaine and 4 mg/mL oxybuprocaine, Colicursi, Alcon). Denucleation of corneal surface was performed by rubbing with a cotton swab soaked in *n*-heptanol (Sigma-Aldrich) for 1 minute followed by a surgical limbal peritomy (180° or 360°). Three weeks after injury, AM without hAT-MSCs was transplanted to the ocular surface of three animals with partial LSCD. AM with hAT-MSCs was transplanted to the ocular surface of 11 animals (six of the partial LSCD model and five of the total LSCD) and sutured with Surgipro II 7.0 polypropylene suture (Tyco Healthcare Group, Cork, Ireland, <http://www.tyco.com>). After transplantation, the eyelids were closed with a partial tarsorrhaphy (leaving enough space to apply topical drugs) using 5.0 silk sutures (AJL Ophthalmic, Álava, Spain, <http://ajlsa.com>). Triamcinolone (40 mg, Trigon Depot, Bristol-Myers Squibb, Madrid, Spain, <http://www.bms.es>) was administered by transeptal injection. Topical anti-inflammatory and antibiotics and systemic analgesics and antibiotics were administered daily for 5 days. Two weeks after the transplantation, the eyelids were re-opened. Eleven weeks after the creation of the injury, the animals were euthanized by intravenous injection of 200 mg/kg pentobarbital sodium (Dolethal, Vetoquinol, Lure, France, <http://www.vetoquinol.com>). Samples of cornea and limbus were collected and fixed in 4% formaldehyde (Panreac, Barcelona, Spain, <http://www.panreac.es>) for histopathology analysis.

Clinical Evaluation

Corneal neovascularization, corneal opacity, and corneal epithelial defects (stained with sodium fluorescein, Colircusi Fluotest, Alcon) were clinically examined weekly by slit lamp (Kowa SL-15, Kowa Medicals, Tokyo, Japan, <http://www.kowamedical.com>) and assessed from 0 to 4 by two different researchers [30]. Neovascularization and epithelial defects were scored using the following scale: 0, none; 1, area $\leq \frac{1}{4}$; 2, $\frac{1}{4} < \text{area} \leq \frac{1}{2}$; 3, $\frac{1}{2} < \text{area} \leq \frac{3}{4}$; and 4, area $> \frac{3}{4}$ (Supporting Information Table S2). In the total LSCD model, conjunctival invasion was similarly evaluated and also measured in millimeters. Additionally, neovessel length was scored in millimeters as well as with the Efron scale [31]. Corneal opacity was scored as follows: 0, none; 1, mild; 2, moderate; 3, severe, pupil seen faintly; and 4, severe, pupil not visible (Supporting Information Table S2). Furthermore, epithelial defect areas were measured by the image-processing program Image J (<http://rsb.info.nih.gov/ij/>). In the total LSCD model, the cornea was divided in five different areas, and each area was scored for each clinical sign.

Histopathology

Histopathological analysis was performed in all eyes at the end of follow-up to evaluate the degree of damage created in the cornea and the limbus and recovery after transplantation. Fixed tissue samples were processed, embedded in paraffin, and cut in 4 μm slices with a microtome. The tissue sections were prepared in the sagittal plane of the central cornea so that each slice included the superior limbus, central cornea, and inferior limbus. In total, 18–20 sections were cut from each sample, and six of them were used for histopathology. The others were used for immunofluorescence microscopy. Periodic acid-Schiff staining was performed to show goblet cells in the limbal or corneal epithelium and inflammatory cells and blood vessels in the corneal and limbal stroma. The healthy contralateral eyes of six rabbits were used as the control group (Group 0). The presence of inflammatory cells was semi-quantified using the following scale: 0, absence; 1, low amount; 2, moderate amount; and 3, high amount.

Immunofluorescence Microscopy

Histological sections were permeabilized with phosphate-buffered saline (PBS) (Life Technologies) containing 0.3% Triton X-100 (Sigma-Aldrich). Afterward, samples were incubated for 1 hour with 5% donkey or goat serum (Sigma-Aldrich) in PBS at room temperature to block nonspecific binding. Following that, they were incubated at 4°C overnight with cell-specific monoclonal antibodies against the corneal epithelial markers CK3 [32] and E-cadherin [33], the limbal epithelial markers CK15 [34] and p63 [35], and the conjunctival epithelial marker CK7 [36] diluted in blocking buffer (Supporting Information Table S3). Afterward, the samples were incubated for 1 hour at room temperature in darkness with the secondary antibody (PECy5 goat anti-mouse) diluted in PBS (Supporting Information Table S3). Immunofluorescence against BrdU (AntiBrdU-DyLight650; Supporting Information Table S3) was performed to locate hAT-MSCs. The samples were first incubated with 2 M HCl (Panreac) at room temperature for 30 minutes to enable access of the antibody to the DNA, and neutralized with sodium borate buffer (10 mM NaOH, pH 8.5). Finally, cell nuclei were counterstained with Hoechst (Sigma-Aldrich) and visualized in an inverted fluorescence microscope (DM4000B Leica, Wetzlar, Germany, <http://www.leica.com>). Primary antibodies were omitted in negative control studies. Samples in which CK7 expression were studied were also incubated with lectin-FITC from Helix Pomatia (1:500, Sigma-Aldrich) for 30 minutes to show goblet cell mucin. The healthy contralateral eyes of six rabbits were used as controls (Group 0). Twelve sections from each experimental group were used to study the expression of each marker. The percentage of p63-positive cells was calculated in the tissues of the different groups.

Statistical Analysis

Under guidance of the IOBA Statistical Unit (Dr. Itziar Fernández), mean \pm SEM values were calculated and analyzed using the Statistical Procedures for the Social Sciences (SPSS 18.0, IBM Corporation, Somers, NY, <https://www.ibm.com>). Two-sided $p \leq .05$ were considered statistically significant. For analysis of qualitative variables, the Kruskal-Wallis test for more than two groups or the Mann-Whitney U test for two groups were used. The Friedman test for more than two groups or the Wilcoxon test for two groups were used to compare values over time. For quantitative data, statistical

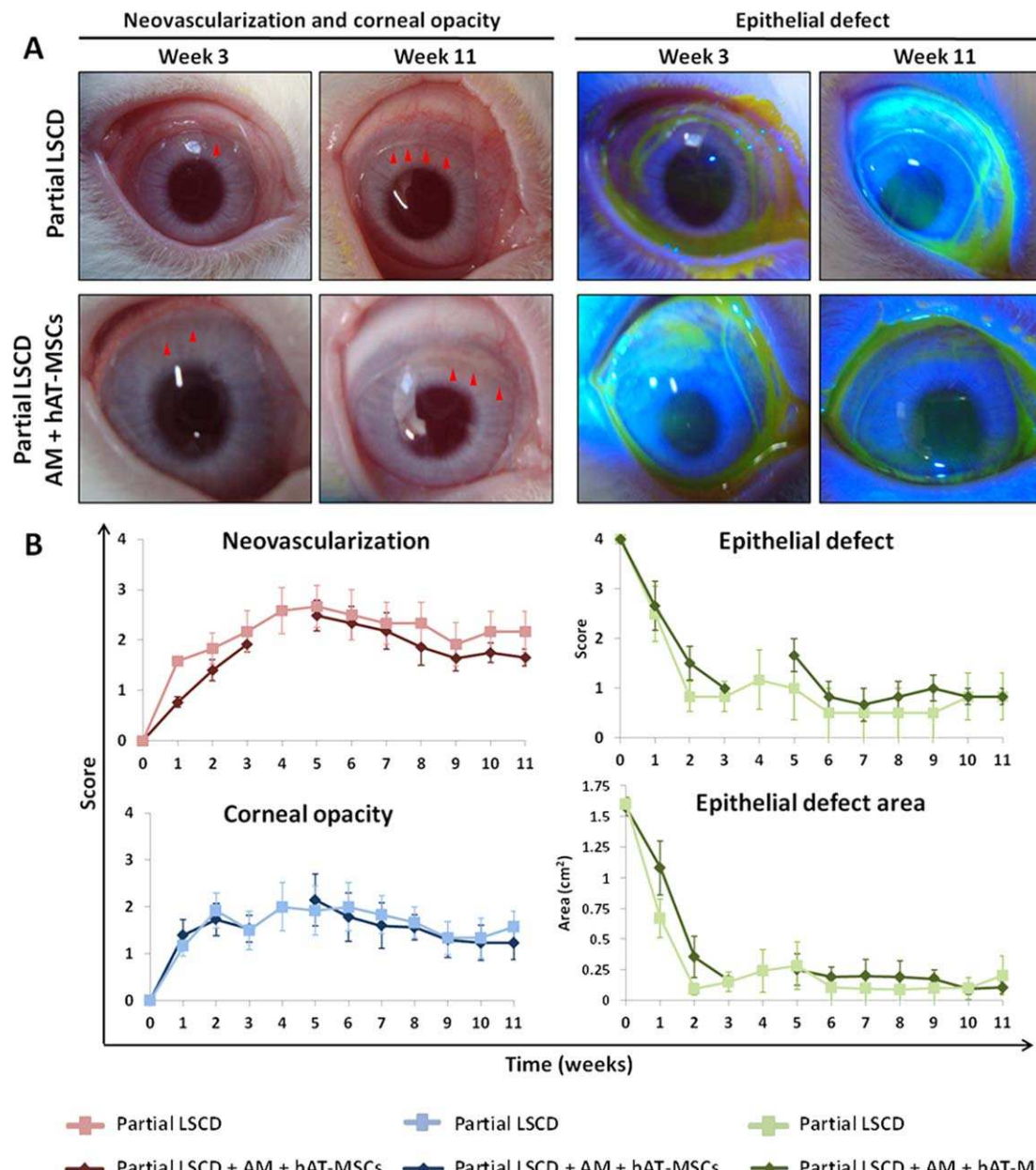


Figure 1. Ocular surface evaluation in the partial limbal stem cell deficiency model without and with human adipose tissue-derived mesenchymal stem cells (hAT-MSCs). **(A)**: Representative images from the control and hAT-MSC transplanted group. Red arrowheads, neovascularization sites. **(B)**: Neovascularization and corneal opacity developed during the first weeks after the creation of the injury. Epithelial defects were partially resolved during the first 2 weeks. The clinical signs did not change after the hAT-MSC transplantation. There were no significant differences between the non-transplanted and the transplanted groups. Data for Week 0 were acquired immediately after the injury. Data for Week 3 were acquired before transplantation. Abbreviations: AM, amniotic membrane; hAT-MSCs, human adipose-derived mesenchymal stem cells; LSCD, limbal stem cell deficiency.

significance was determined by two-way factorial repeated measures analysis of variance. The comparison between two groups was made using Student's *t* test. Spearman's correlation coefficients were used to correlate the presence of inflammatory cells and hAT-MSCs.

RESULTS

Clinical Analysis

Partial LSCD Model. In the partial LSCD model, where the limbectomy was localized to the superior and temporal

limbus, neovascularization and corneal opacity were present from 1 week after injury (Fig. 1A, 1B). The neovessels appeared mainly in the superior area of the cornea. Epithelial defects were partially resolved during the first 2 weeks (Fig. 1B). Three weeks after injury, AMs without cells were transplanted to the ocular surface of three rabbits, and AMs with hAT-MSCs were transplanted to six rabbits. There were no differences in clinical signs between rabbits in the partial LSCD model without treatment and those transplanted with AM but without hAT-MSCs (Supporting Information Fig. S1). In the six animals of the AM + hAT-MSC transplanted group, before transplantation, neovessels covered between $\frac{1}{4}$ and $\frac{1}{2}$ of the

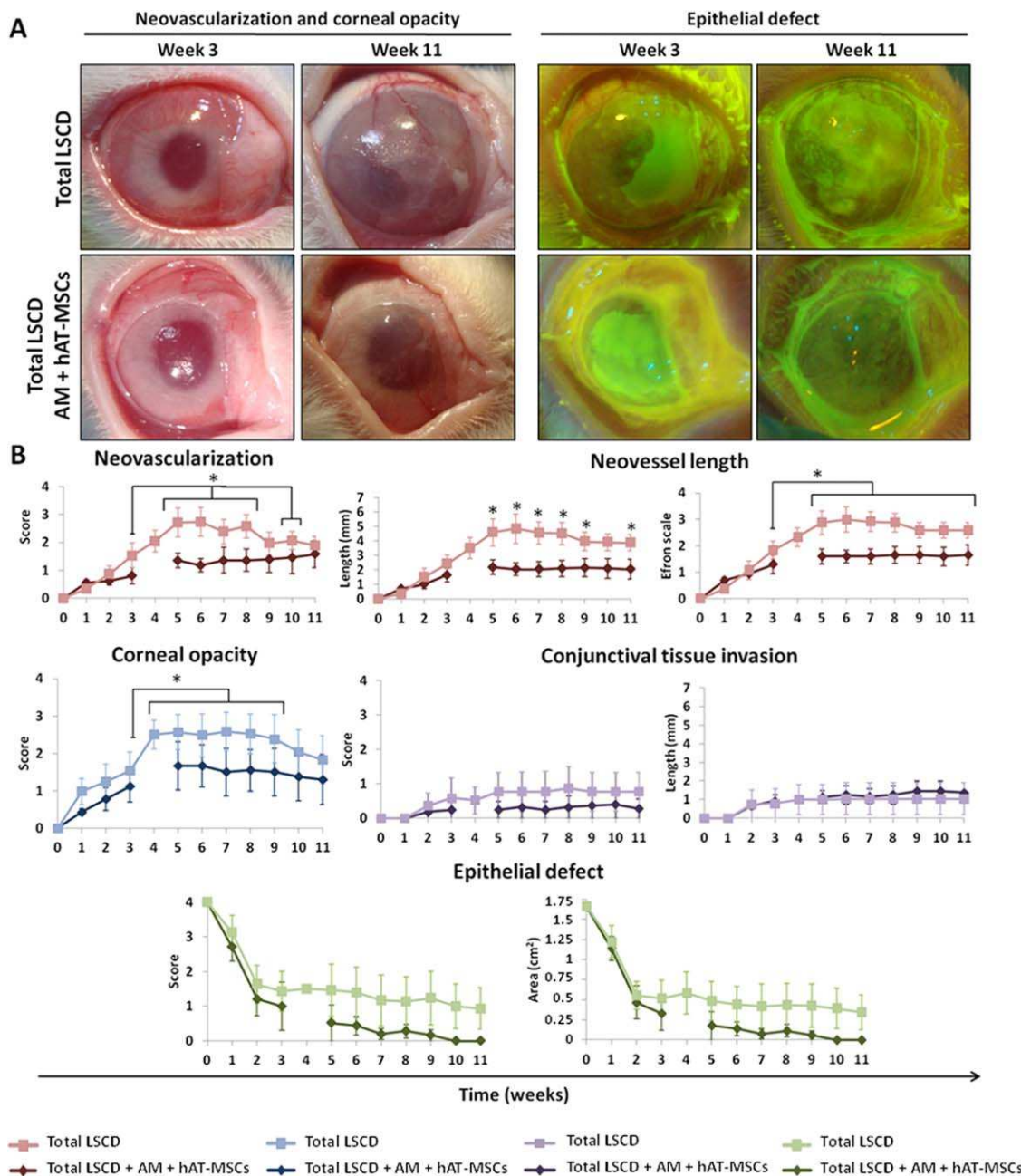


Figure 2. Ocular surface evaluation in the total limbal stem cell deficiency (LSCD) model without and with human adipose tissue-derived mesenchymal stem cells (hAT-MSCs). **(A)**: Representative images from the control and hAT-MSC transplanted group. **(B)**: In the control total LSCD group, there was a significant increase in neovascularization, neovessel length, and corneal opacity after Week 3. However, these clinical signs did not increase after hAT-MSC transplantation. Neovessel length was higher in the control group than in the hAT-MSC transplanted group. Two of the six animals of the control group, and one of the five animals of the transplanted group had a thick conjunctival invasion on the corneal surface, but overall it was not significant. Data for Week 0 were acquired immediately after the creation of the injury. Data for Week 3 were acquired before transplantation. *, p ≤ .05. Abbreviations: AM, amniotic membrane; hAT-MSCs, human adipose tissue-derived mesenchymal stem cells; LSCD, limbal stem cell deficiency.

total cornea, corneal opacities were moderate, and epithelial defects were smaller than $\frac{1}{4}$ of the total cornea. The clinical signs did not change after the hAT-MSC transplantation (Fig. 1). While there were no significant differences between the non-transplanted and the AM + hAT-MSC transplanted group with respect to neovascularization, corneal opacity, and epithelial defects (Fig. 1), these results indicated that hAT-MSCs

were well tolerated on the ocular surface of the partial LSCD model.

Total LSCD Model. In rabbits with total LSCD, neovascularization and corneal opacity developed during the first weeks after the injury (Fig. 2A, 2B). Epithelial defects partially

recovered during the first 2 weeks (Fig. 2B). Three weeks after the creation of the injury, hAT-MSCs seeded onto AMs were transplanted to the ocular surface of five rabbits (one animal was excluded for transplantation because it developed a symblepharon, an adhesion of the palpebral conjunctiva to the bulbar conjunctiva). In the total LSCD group without treatment, there was a significant increase in neovascularization, especially between Week 3 and Weeks 5, 6, 7, 8, and 10 ($p = .046$, $p = .043$, $p = .028$, $p = .028$, and $p = .046$, respectively; Fig. 2B). However, the increase in neovascularization was not present after hAT-MSC transplantation. Neovessel length was higher in the total LSCD group without treatment than in the hAT-MSC transplanted group during Weeks 5, 6, 7, 8, 9, and 11 ($p = .041$, $p = .034$, $p = .011$, $p = .012$, $p = .046$, and $p = .04$, respectively; Fig. 2B). Furthermore, when vessel length was scored on the Efron scale, there was a significant increase in length for the non-transplanted group between Week 3 and Weeks 5–11 ($p = .042$, $p = .028$, $p = .028$, $p = .027$, $p = .028$, $p = .028$, and $p = .028$, respectively), whereas in the transplanted group, this increase was not present (Fig. 2B).

There was an increase in corneal opacity from Week 3 to Weeks 4–9 ($p = .028$, $p = .028$, $p = .028$, $p = .028$, $p = .028$, and $p = .046$, respectively) in the non-transplanted group (Fig. 2B), but this was absent from the hAT-MSC transplantation group. In the non-transplanted group, there was a thick conjunctival invasion on the corneal surface in two of the six animals. A similar invasion occurred in only one of the five animals in the transplanted group. However, the conjunctival invasion on the cornea was not statistically significant in any of the groups (Fig. 2B). While the epithelial defect scores and areas for the non-transplanted group were greater than for the transplanted group, the differences were not statistically significant (Fig. 2B). Collectively, these results indicated that hAT-MSC transplantation prevented the progression of LSCD (Fig. 2).

Histopathology

Partial LSCD Model. At the end of the follow-up at Week 11, 4–5 epithelial layers were present in the central cornea and 6–7 in the superior and inferior limbus of the control non-LSCD eyes (Fig. 3). The same number of layers was also present in the partial LSCD group without treatment. Goblet cells, which are present in the normal conjunctival epithelium but not in the cornea or limbus, occurred in the superior and inferior limbal epithelium of the untreated partial LSCD model. They were also present in the limbus of eyes transplanted with AM and transplanted with AM + hAT-MSCs (Fig. 3). Inflammatory lymphocytes were present in the superior and inferior limbal stroma of the untreated partial LSCD eyes, partial LSCD eyes with AM, and partial LSCD eyes with AM + hAT-MSCs. However, the central cornea of all groups was normal in appearance, containing no goblet cells, inflammation, or neovessels. There were no histological differences among the three groups of the partial LSCD model. Furthermore, there were no adverse reactions in the tissues after the transplantation of AM + hAT-MSCs, which confirmed that the ocular surface was highly tolerant of these cells (Fig. 3; Supporting Information Fig. S2).

Total LSCD Model. In the untreated total LSCD group at the end of the follow-up at Week 11, there were only 2–3

epithelial layers in the central cornea compared with the 4–5 layers in the non-LSCD control eyes (Fig. 3). Similarly, the 2–3 epithelial layers in the limbus were less than the 6–7 layers present in the non-LSCD eyes. Furthermore, the epithelium of the non-transplanted eyes was disorganized, and goblet cells were present in the superior and inferior limbal epithelium, indicating the occurrence of conjunctival in-growth (Fig. 3). In two of the six untreated animals with total LSCD, goblet cells were present in the central cornea. Inflammatory cells (lymphocytes) and disorganization of the stromal fibers in the superior and inferior limbal stroma and in the central cornea demonstrated that the total LSCD model was more severe than the partial LSCD model.

As in the non-transplanted group, the AM + hAT-MSC transplanted group at Week 11 had fewer epithelial layers than in the healthy tissues. Moreover, goblet cells were present in the limbal epithelium and inflammatory cells were in the limbal stroma. In one of the animals, goblet cells and inflammation were also noted in the central cornea. However overall, the hAT-MSC transplanted eyes had fewer inflammatory cells and less disorganization in the stroma of the central cornea in comparison with the non-transplanted group (Fig. 3; Supporting Information Fig. S2).

hAT-MSC Localization

The hAT-MSCs labeled with BrdU were located in the inflamed areas of the superior and inferior limbal stroma 8 weeks after transplantation in both partial and total LSCD models (Fig. 3; Supporting Information Fig. S2). The eyes with a more prominent inflammatory infiltrate also had more hAT-MSCs. The hAT-MSCs were located in the central cornea of the animals with inflammation in this area. The correlation between the amount of hAT-MSCs transplanted and the level of inflammation in the cornea was significant ($r = 0.810$; $p = .003$; Supporting Information Fig. S2).

Phenotypic Analysis

The presence of five phenotype-specific marker proteins was assessed at the end of the 11-week follow-up period. The presence of CK3, a specific marker of corneal epithelial cells [32], increased in the limbal epithelium of the untreated partial LSCD model (Fig. 4). However, in the partial LSCD model transplanted with AM, the expression of CK3 was reduced. In the partial LSCD model transplanted with hAT-MSCs, CK3 expression was similar to the healthy control eyes. CK3 was not expressed in the epithelium of the untreated total LSCD model (Fig. 4). However, it was expressed in the corneal and limbal epithelia of the total LSCD model transplanted with AM + hAT-MSCs (Fig. 4; Supporting Information Table S4).

The expression of E-cadherin, another marker of corneal epithelial cells [33], did not change in the partial LSCD model (Fig. 5). In the untreated total LSCD model, E-cadherin was not expressed. However, it was present in the corneal and limbal epithelia of the total LSCD model transplanted with AM + hAT-MSCs (Fig. 5; Supporting Information Table S4).

CK15 (Fig. 6) and p63 (Fig. 7), markers of limbal epithelial stem cells [34, 35], were lost in the damaged superior limbus of the untreated partial LSCD model and in the partial LSCD eyes transplanted with AM alone. However, expression of both markers was partially restored in the superior limbus of

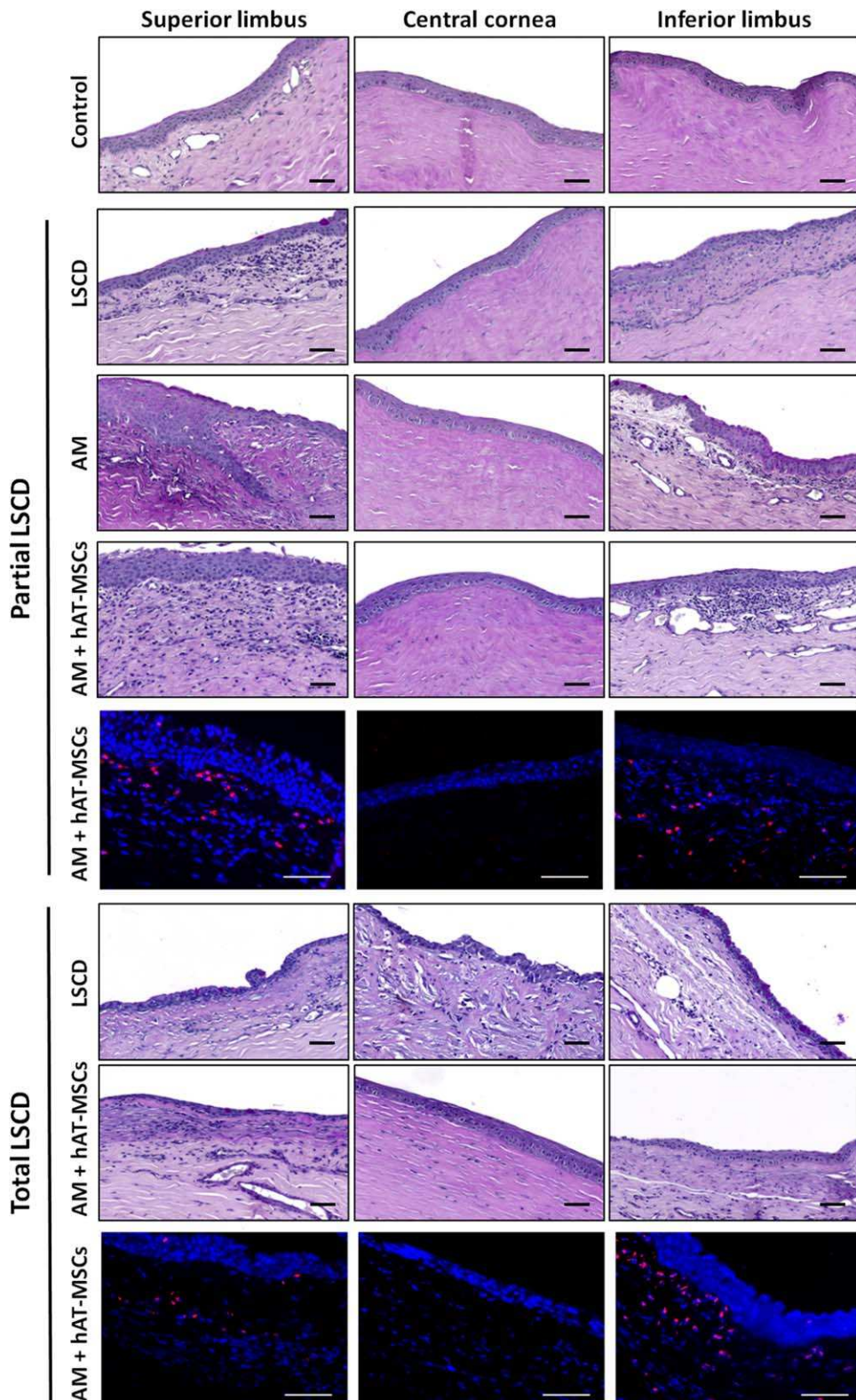


Figure 3. Periodic acid-Schiff and 5'-bromo-2'-deoxyuridine (BrdU) staining in control, partial limbal stem cell deficiency (LSCD), and total LSCD eyes with and without amniotic membrane (AM) or AM + human adipose tissue-derived mesenchymal stem cell (hAT-MSC) transplants. Goblet cells (purple) in the limbal epithelium and inflammatory cells (dark purple) were present in the limbal stroma of the five study groups (partial LSCD without treatment, partial LSCD with AM, partial LSCD with hAT-MSCs, total LSCD without treatment, and total LSCD with hAT-MSCs) at the end of the follow-up period (11 weeks). In the partial LSCD model, there were no differences between the non-transplanted and the transplanted groups. In the total LSCD model, the non-transplanted group presented fewer epithelial layers, a disorganized cornea (epithelium and stroma) and inflammatory cells in the stroma of the central cornea. However, the hAT-MSC transplanted eyes had fewer inflammatory cells and less disorganization in the stroma of the central cornea. BrdU-containing hAT-MSCs (red) were located in the inflamed areas of the limbal stroma (superior and inferior) 8 weeks after transplantation in both partial and total LSCD models. Blue, nuclei. Scale bar = 50 μ m. Abbreviations: AM, amniotic membrane; hAT-MSCs, human adipose-derived mesenchymal stem cells; LSCD, limbal stem cell deficiency.

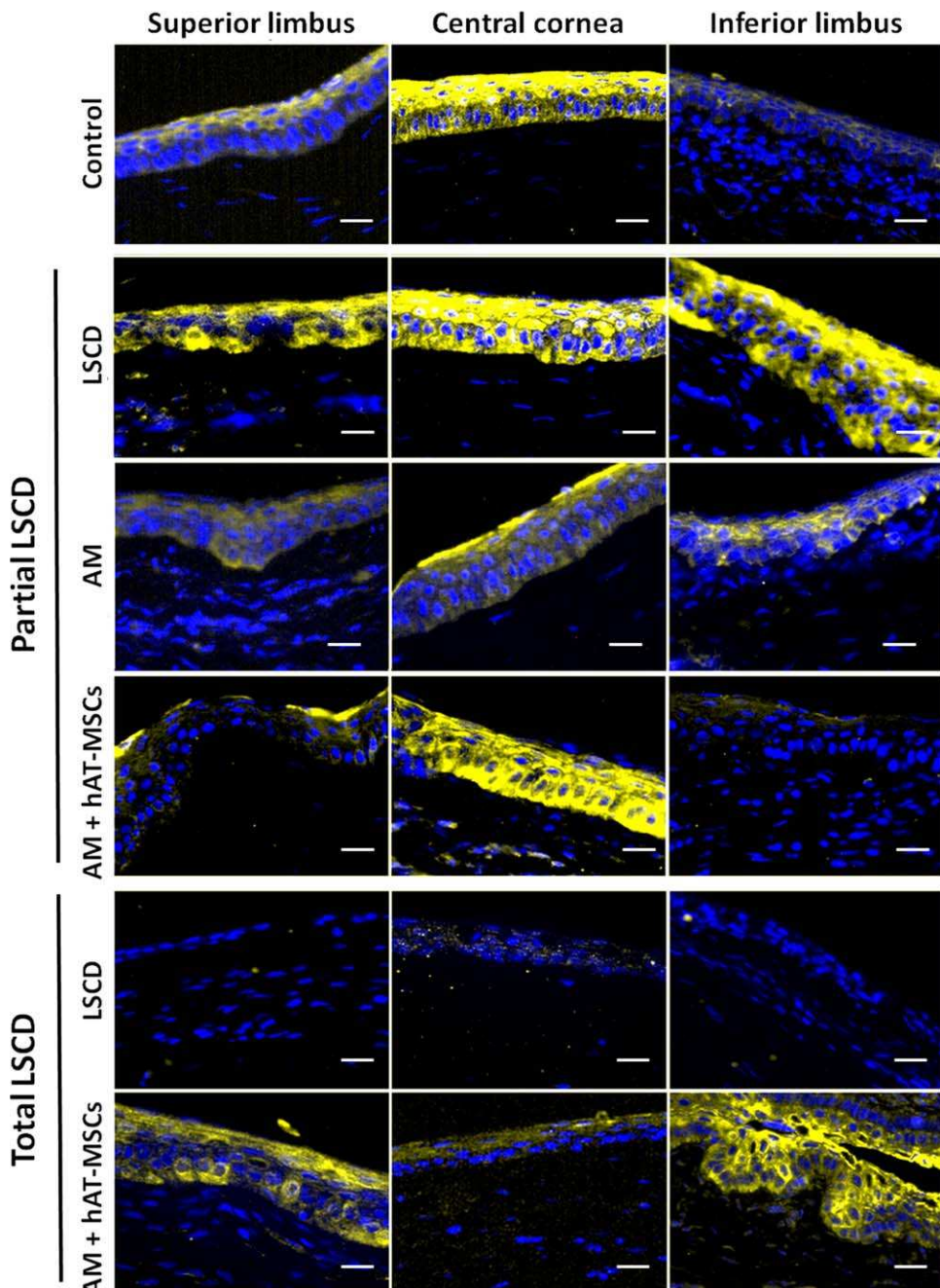


Figure 4. Immunofluorescence microscopy of CK3 expression, a corneal epithelial marker, in the ocular surface of the partial and total limbal stem cell deficiency (LSCD) models at the end of the follow-up period. Compared with the control, CK3 expression (yellow) increased in the limbal epithelium of the untreated partial LSCD model. In the partial LSCD model transplanted with amniotic membrane (AM), the expression of CK3 was reduced in the corneal epithelium. However, in the partial LSCD model after the AM + human adipose tissue-derived mesenchymal stem cell (hAT-MSC) transplantation, it was similar to the healthy control group. CK3 was not expressed in the epithelium of the untreated total LSCD model. However, it was expressed in the corneal and limbal epithelia of the total LSCD model transplanted with AM + hAT-MSCs. Nuclei, blue. Representative images from each group. Scale bar = 100 μ m. Abbreviations: AM, amniotic membrane; hAT-MSCs, human adipose-derived mesenchymal stem cells; LSCD, limbal stem cell deficiency.

the partial LSCD transplanted with AM + hAT-MSCs (Supporting Information Table S4; Fig. S3). In the limbal epithelium of the healthy control eyes, the percentage of p63-positive cells was $47.7\% \pm 3.7\%$ ($45.5\% \pm 3.1\%$ in the superior limbus and $50.1\% \pm 7.3\%$ in the inferior limbus). In the limbal epithelium of the partial LSCD model, the percentage of p63-positive cells was significantly lower than in the control healthy group

($16\% \pm 3.3\%$ vs. $47.7\% \pm 3.7\%$; $p < .001$). This decrease was higher in the damaged area (superior limbus, $3\% \pm 2\%$; $p < .001$) than in the inferior limbus ($25.6\% \pm 4\%$; $p = .006$) in comparison with the same area of the control group. Very similar results were observed in the limbal epithelium of the animals transplanted with cell-free AM. The percentage of p63-positive cells was $16.6\% \pm 5.9\%$ in the total limbus,

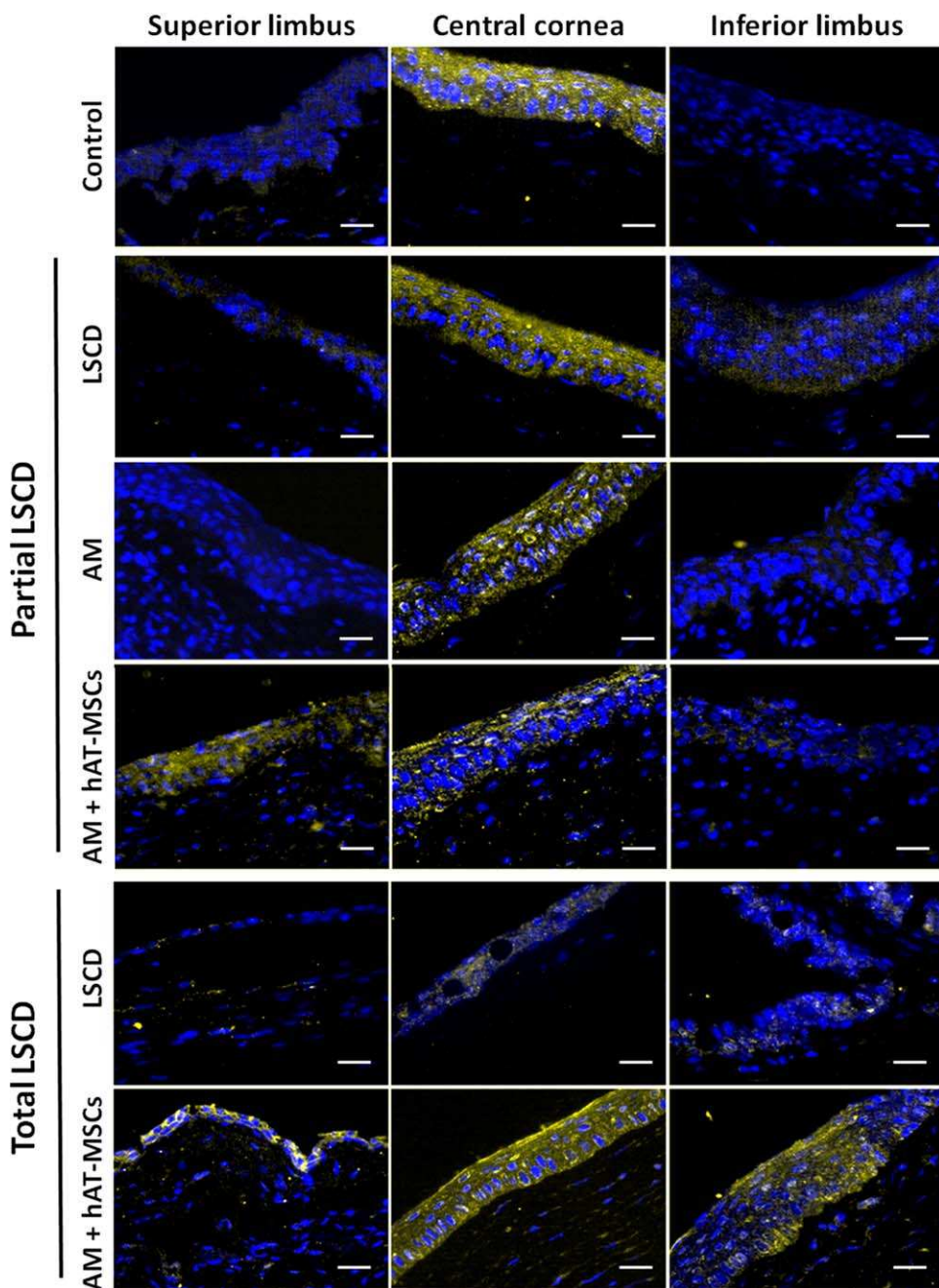


Figure 5. Immunofluorescence microscopy of E-cadherin expression, a corneal epithelial cell marker, in the ocular surface of the partial and total limbal stem cell deficiency (LSCD) models at the end of the follow-up period. Compared with the control, the expression of E-cadherin (yellow) did not change in the partial LSCD model. In the untreated total LSCD model, E-cadherin was not expressed, but it was present in the corneal and limbal epithelia of the total LSCD model transplanted with amniotic membrane + human adipose tissue-derived mesenchymal stem cells. Nuclei, blue. Representative images from each group. Scale bar = 100 μ m. Abbreviations: AM, amniotic membrane; hAT-MSCs, human adipose-derived mesenchymal stem cells; LSCD, limbal stem cell deficiency.

4.8% \pm 2.2% in the superior limbus, and 37.8% \pm 11.1% in the inferior limbus. These percentages were significantly lower than for the healthy control group in the total limbus ($p = .001$) and in the superior limbus ($p < .001$), but not different for the inferior limbus or in comparison with the untreated group. The expression of positive cells for p63 was significantly lower in the hAT-MSC transplanted group in comparison with the healthy control group (35.7% \pm 1.8% vs. 47.7% \pm 3.7%, $p = .038$). However, the expression of p63 was

partially restored in the hAT-MSC transplanted group (35.7% \pm 1.8%), especially in the superior limbus (36.3% \pm 2.7%), showing a significant increase in comparison with the untreated group ($p < .001$ for total and superior limbus) and with the AM-transplanted group ($p = .032$ for total limbus and $p < .001$ for superior limbus) (Supporting Information Fig. S3). In the total LSCD model, the expression of CK15 (Fig. 6) and p63 (Fig. 7; Supporting Information Fig. S3) was lost in the limbal epithelium, but it was partially recovered in the AM + hAT-MSC

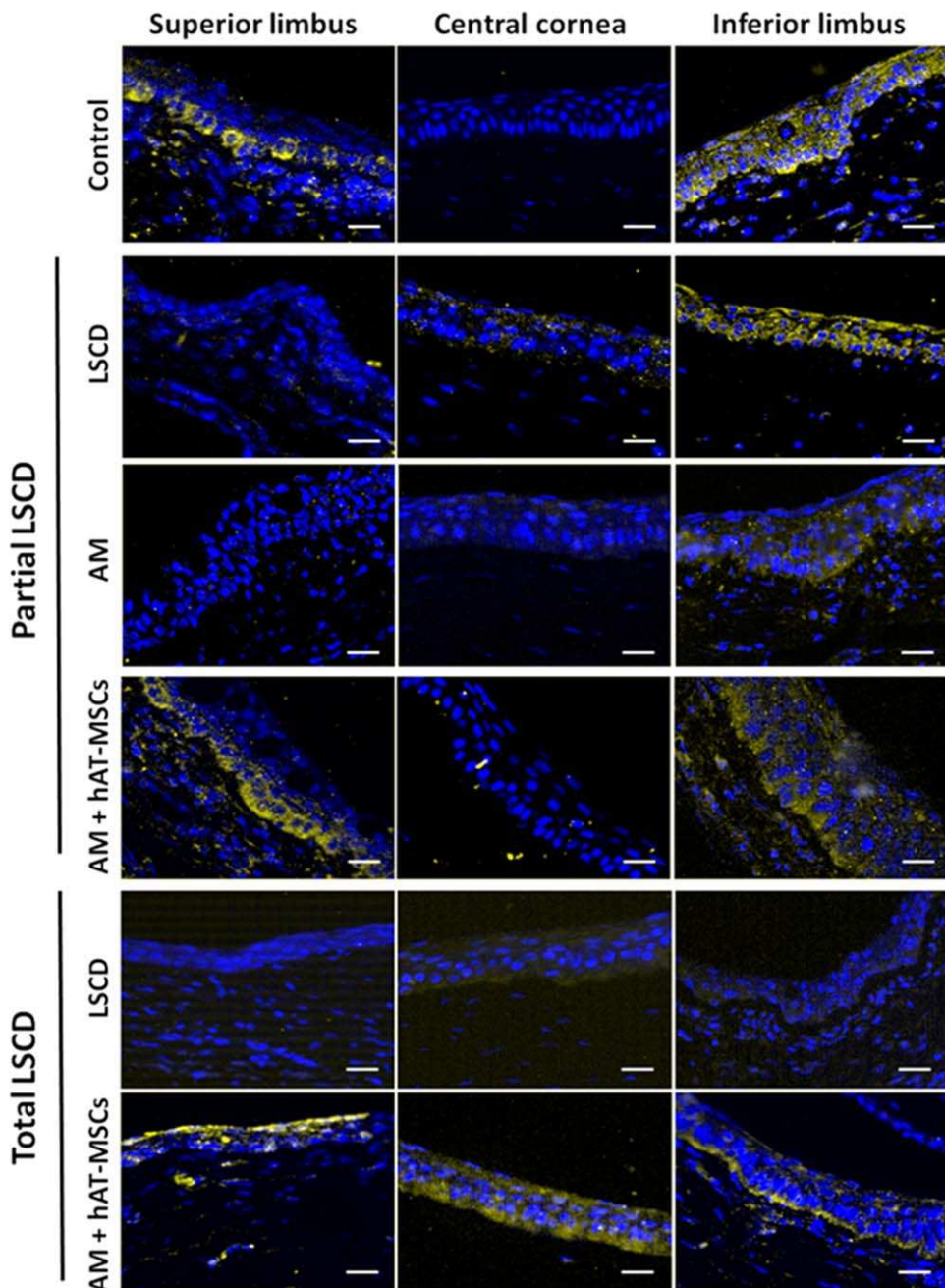


Figure 6. Immunofluorescence microscopy of CK15 expression, a limbal stem cell marker, in the ocular surface of the partial and total limbal stem cell deficiency (LSCD) models at the end of the follow-up period. CK15 expression (yellow) was lost in the damaged superior limbus of the untreated partial LSCD model and in those transplanted with amniotic membrane (AM). There was a partial recovery in the human adipose tissue-derived mesenchymal stem cell (hAT-MSC) transplanted group. In the total LSCD model, the expression of CK15 was lost in the limbal epithelium, but it was partially recovered in the corneal and limbal epithelia of the AM + hAT-MSC transplanted group. Nuclei, blue. Representative images from each group. Scale bar = 100 μ m. Abbreviations: AM, amniotic membrane; hAT-MSCs, human adipose-derived mesenchymal stem cells; LSCD, limbal stem cell deficiency.

transplanted group (Supporting Information Table S4; Fig. S3). Additionally, CK15 was expressed in the corneal epithelium of the AM + hAT-MSC transplanted group. In the total LSCD model, the percentage of p63-positive cells was significantly lower in the untreated group than in the healthy control group ($3.7\% \pm 1.2\%$ vs. $47.7\% \pm 3.7\%$ in the total limbus, $p < .001$; $4.5\% \pm 2.1\%$ vs. $45.5\% \pm 3.1\%$ in the superior limbus, $p < .001$; and $2.9\% \pm 1.4\%$ vs. $50.1\% \pm 7.3\%$ in the inferior limbus, $p = .001$). The hAT-MSC transplanted group had a lower percentage of cells expressing

p63 than the healthy control group ($19.1\% \pm 3.6\%$ vs. $47.7\% \pm 3.7\%$ in the total limbus, $p < .001$; $13\% \pm 2.5\%$ vs. $45.5\% \pm 3.1\%$ in the superior limbus, $p = .001$; and $24.7\% \pm 6.3\%$ vs. $50.1\% \pm 7.3\%$ in the inferior limbus, $p = .044$). However, the percentage of p63-positive cells was partially restored in the hAT-MSC transplanted group, especially in the inferior limbus, in comparison with the untreated group ($p = .001$ for total limbus, $p = .048$ for superior limbus, and $p = .011$ for inferior limbus) (Supporting Information Fig. S3).

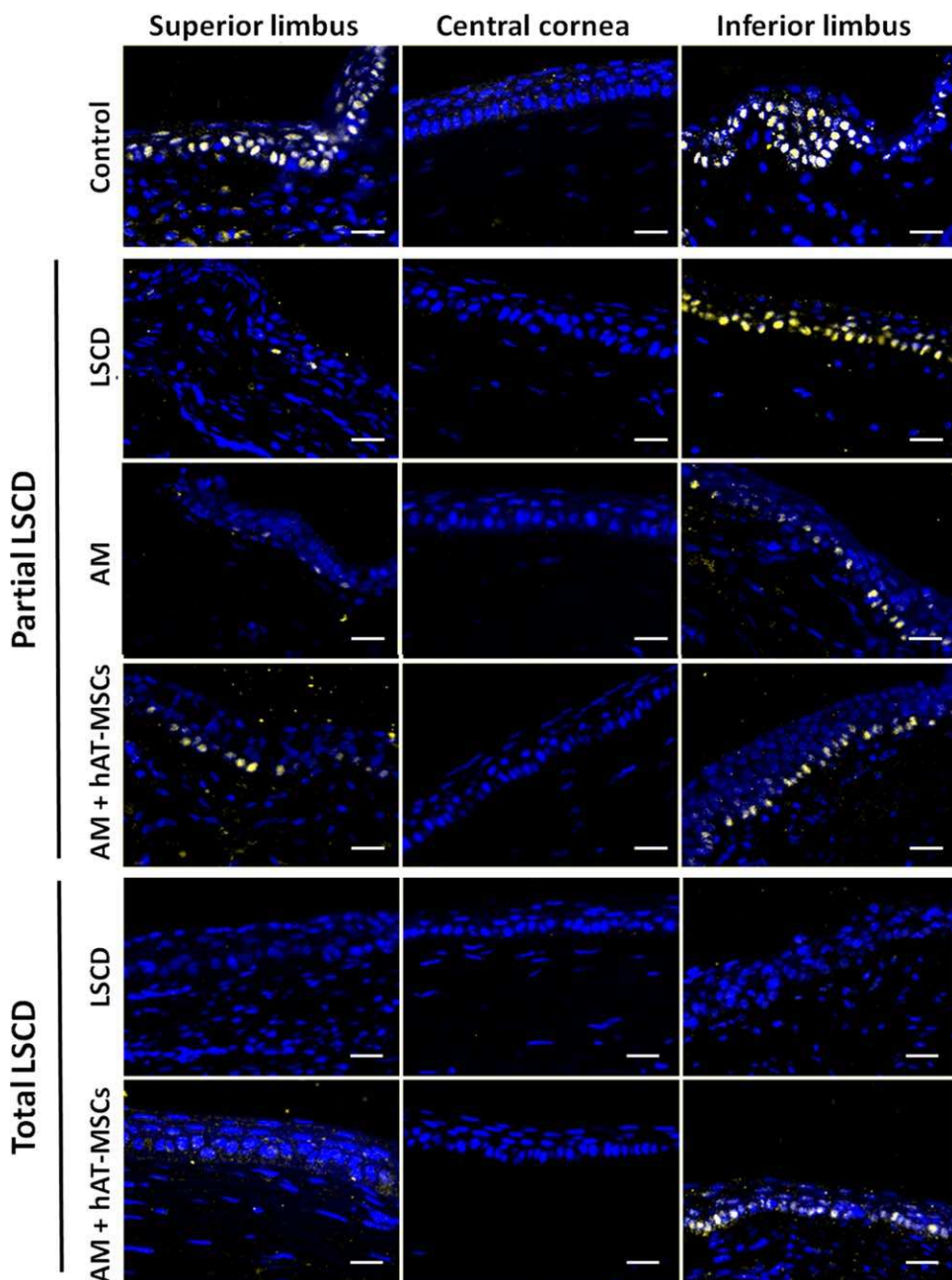


Figure 7. Immunofluorescence microscopy of p63 expression, a limbal stem cell marker, in the ocular surface of the partial and total limbal stem cell deficiency (LSCD) models at the end of the follow-up period. The expression of p63 (yellow) was lost in the damaged superior limbus of the untreated partial LSCD model and in the amniotic membrane (AM)-transplanted eyes. There was partial recovery in the AM + human adipose tissue-derived mesenchymal stem cell (hAT-MSC) transplanted group. In the total LSCD model, p63 expression was lost in the limbal epithelium, but it was partially recovered in the AM + hAT-MSC transplanted group. Nuclei, blue. Representative images from animals of each group. Scale bar = 100 μ m. Abbreviations: AM, amniotic membrane; hAT-MSCs, human adipose-derived mesenchymal stem cells; LSCD, limbal stem cell deficiency.

The conjunctival epithelial cell marker CK7 [36] was expressed in the conjunctival epithelium and in some cells of the limbal epithelium in the healthy eyes (Supporting Information Fig. S4). There were no differences in CK7 expression among the different control and experimental groups of the partial and total LSCD models (Supporting Information Fig. S4; Table S4). Mucins in goblet cells stained by lectin were present in the conjunctiva while some were located in the limbus of healthy eyes. Additionally, there was a diffuse staining on

the surface of the conjunctival and limbal epithelia, indicating the presence of secreted mucins. Except as noted below, there were no differences in the staining of mucins by lectin among the different control or experimental groups of either the partial and total LSCD models. In the partial LSCD model, the central cornea remained free of lectin-stained goblet cells. In two of the six animals with untreated total LSCD, goblet cells were present in the central cornea. However, only one animal of the total LSCD group transplanted with AM + hAT-

MSCs had goblet cells in the central cornea (Supporting Information Fig. S4).

DISCUSSION

To study the tolerance and efficacy of the hAT-MSCs transplanted onto the ocular surface, it was first necessary to develop an *in vivo* experimental model that closely resembles human LSCD disease. To that end, we used surgical limbectomy to develop two different rabbit models that mimicked the progressive LSCD grades of severity in humans. We chose rabbit to develop our models because the rabbit cornea is large enough to perform surgeries, the histological structures of the eye are similar to human eyes [37], and many of the *in vivo* LSCD models have been developed using rabbits [38–40].

By performing a *n*-heptanol-based denudation of the corneal surface followed by a surgical 180° limbectomy in the superior and temporal ocular surface quadrants, we developed a partial, mild LSCD model. Clinically and pathologically, the model resembled mild LSCD in humans [4, 5]. In our rabbits, neovascularization and corneal opacification occurred during the first 3 weeks after the generation of the injury, but the epithelial defects arising from the heptanol denudation of the cornea partially recovered during the first 2 weeks, as also described by Chen and Tseng [41]. In our study, from the third week after induction of partial LSCD, even in the absence of further treatment, the clinical signs became stable and were maintained throughout the follow-up. Based on these findings and those of others [42], we selected the third week for the time of transplantation.

We generated a total LSCD model by performing *n*-heptanol-based denudation of the corneal surface followed by a 360° limbectomy. This model clinically and pathologically resembled moderate-to-severe LSCD in humans [4, 5]. Neovascularization and corneal opacification were more severe than in the partial LSCD, and they developed over the first 3 weeks after the creation of the injury, as other authors have noted [23, 43–45]. Moreover, the epithelial defects underwent partial recovery during the first 2 weeks and were maintained during the follow-up period, as reported by others [30, 46]. In two of the six untreated rabbits, a thick conjunctival invasion occurred on the corneal surface, indicating that the total LSCD model was more severe than the partial LSCD model, as we expected. In addition, these results confirm that the limbus acts as a physical barrier between the conjunctiva and the cornea.

AMs without cells were transplanted to the ocular surface of three rabbits with partial LSCD to make sure that an adverse reaction would not occur after surgical suturing. The clinical signs did not change after the AM transplantation in comparison with the partial LSCD group without AM. Due to the lack of changes in the clinical signs after the AM transplantation, we decided that it was not necessary to include a group transplanted with cell-free AM in the total LSCD model. According to our results, previous *in vivo* studies did not find significant differences in the evolution of clinical signs in animals with untreated LSCD or when treated with cell-free AM [40, 47]. Nevertheless, due to its re-epithelializing, anti-inflammatory, antifibrotic, and anti-angiogenic properties, cell-free

AM transplantation is a procedure frequently performed in patients with mild and/or partial LSCD to improve their clinical situation [48, 49]. However, cell-free AM transplantation is insufficient for regeneration of the ocular surface in patients with severe and/or total LSCD [50].

The clinical signs did not improve in the partial LSCD model after hAT-MSC transplantation. The mildness of the model could partially explain this lack of improvement. However, the fact that the clinical signs did not increase after the hAT-MSC transplantation indicates that hAT-MSCs were well tolerated in the rabbit ocular surface even without the use of immunosuppression. These results agree with other studies in which human MSCs were transplanted to the ocular surface of mice [21], rats [22, 51], and rabbits [20, 24] without any indications of rejection.

In eyes with total LSCD, the evolution of neovascularization and corneal opacification was restrained after hAT-MSC transplantation. Although a proangiogenic role has been described for MSCs [52], these cells seem to have anti-angiogenic properties in the ocular surface. Decreases in neovascularization and corneal opacity have been previously demonstrated after the hAT-MSC administration [23–25]. In addition, several authors have described the improvement of these clinical signs after MSC administration by different routes [25, 51, 53–56]. While the epithelial defects were larger in the non-transplanted group than in the transplanted group throughout the follow-up period, the differences were not statistically significant. However, other authors have noted that hAT-MSCs contribute to the recovery of corneal epithelium, even in humans [20–26]. Perhaps if the number of animals had been higher, significant differences in epithelial defects would have been more apparent between the different experimental groups.

The presence of inflammatory cells was higher in the limbal stroma of the total LSCD model than in the partial LSCD model. In addition, the stroma was more disorganized in the total LSCD model, indicating again that the total model was more severe than the partial model, as shown by the clinical evaluation. These data suggest that the partial limbectomy produced a mild model of LSCD in rabbits. There were no histological differences among the study groups of the partial LSCD model. However, in the total LSCD model, there was a decrease of inflammatory cells and an improvement of the stromal organization in the AM + hAT-MSC transplanted group. These findings are consistent with the anti-inflammatory role of hAT-MSCs delivered by different routes for corneal chemical burn or in LSCD animal models [21–25]. Moreover, BM-MSCs or MSCs isolated from the limbal stroma can reduce the inflammation in the ocular surfaces [25, 55, 57, 58]. Some of the molecules that are implicated in this anti-inflammatory process are interleukin-10, transforming growth factor- β , and Tumor necrosis factor-stimulated gene 6 (TSG-6) [57, 59, 60].

Goblet cells were present at the end of the follow-up in the limbal epithelium of both partial and total LSCD models. They were also present in the central cornea of three rabbits from the total LSCD model (two in the non-transplanted group; one in the hAT-MSC transplanted group), corresponding with the thick conjunctival invasion of the corneal surface. In general, at the end of the follow-up period, few goblet cells were noted in the corneal epithelium of all study groups. Our results are consistent with the decrease in goblet cell

numbers described for human chemical burns [61] and in rabbits in the weeks after chemical injury [40, 62].

In both the partial and total LSCD models, hAT-MSCs migrated to areas of the limbal stroma that contained many inflammatory cells. Our results are consistent with the migration of topically applied hAT-MSCs to the burned cornea and limbus as described by other authors [21, 22]. Other groups have also demonstrated the migration of limbal stromal MSCs or BM-MSCs to the damaged cornea and limbus when they were applied by different routes [55, 58, 63]. On the other hand, some studies have reported that AT-MSCs or BM-MSCs administered by subconjunctival injection did not migrate away from the injection site [21, 43]. Furthermore, some reports indicated that MSCs administered systemically or intraperitoneally in a LSCD model exert their therapeutic action without migration to the damaged area [59]. One of the well-known signaling pathways that regulate cell homing is mediated by C-X-C motif chemokine 12 or stromal cell-derived factor 1 (CXCL12/SDF-1) and its receptor C-X-C chemokine receptor type 4 (CXCR4), which is expressed by MSCs [64]. Under inflammatory conditions, tissues secrete CXCL12/SDF-1 that attracts MSCs [65]. In normal conditions, CXCL12/SDF-1 is more abundant in the limbal than in the corneal epithelium, and CXCR4 is expressed in the limbal stroma rather than in the corneal stroma [66, 67]. Although there is a lack of data about the expression of these molecules in inflamed ocular surface tissues, these factors could be implicated in the migration of the AT-MSCs to the damaged cornea and limbus of our *in vivo* models.

In our LSCD models, we analyzed by immunofluorescence microscopy the molecular changes in the expression profiles of corneal, limbal, and conjunctival cell markers. The expression of the corneal epithelial cell marker CK3 increased in the limbus of the partial LSCD model, indicating the possibility that limbal epithelial stem cells were differentiating and migrating from the limbus to the central cornea during the restoration of the corneal epithelium. In contrast, the expression of CK3 decreased in the cornea of the untreated total LSCD model in agreement with the data published by other authors using different LSCD models [30, 46, 51, 68].

Although there were no clinical or histological differences between the partial LSCD group without treatment and the AM + hAT-MSC transplanted group, there were some molecular changes. After AM + hAT-MSC transplantation, CK3 was expressed not only in the corneal epithelium, but also in the limbal epithelium. These data suggest that hAT-MSCs contribute to recovery of the corneal epithelium by secreting factors that promote the proliferation and differentiation of the remaining limbal epithelial stem cells. This is consistent with the increased expression of CK3 and/or CK12 in the corneal epithelium after BM-MSC administration in corneal burn and LSCD models [40, 51].

The expression of E-cadherin, an intercellular junction protein, decreased in the total LSCD model, indicating a possible loss of intercellular junctions of the corneal epithelium. Our results are consistent with the decrease in E-cadherin expression similar to that which occurs in defective development of mouse corneal epithelium [69]. E-cadherin expression increased in both the corneal and limbal epithelia of the total

LSCD group transplanted with AM + hAT-MSCs. These data indicate that hAT-MSCs contribute to the recovery of the corneal epithelium. Similarly, the expression of connexin 43, a gap junction protein, occurs after BM-MSC transplantation in a different rabbit model of LSCD [40].

The expression of the limbal epithelial stem cell markers CK15 and p63 was lost from the superior limbus of the partial LSCD model and from the superior and inferior limbus of the total LSCD model, as we expected. The loss of limbal stem cell markers occurs in other LSCD models [51, 70]. However, the expression of CK15 and p63 recovered in the limbal epithelium of the partial and total LSCD groups after AM + hAT-MSC transplantation, like that noted for p63 after BM-MSC transplantation in different LSCD models [51, 71]. However, Reinshagen et al. did not find any differences in corneal p63 expression after the transplantation of BM-MSCs in rabbits with LSCD [40].

Although some authors have proposed the transdifferentiation of MSCs into CK3-expressing corneal epithelial cells [21, 40, 51, 72], only two have demonstrated that MSCs transplanted *in vivo* expressed CK3 in the corneal epithelium [21, 72]. However, we and other authors have shown that MSCs express CK3 in normal culture conditions; thus the CK3 expression might not indicate a real transdifferentiation [18, 40]. Our results, together with those obtained by other authors, indicate that MSCs contribute to the recovery of the corneal epithelium by secreting factors that act at a paracrine level rather than by a transdifferentiation process. These factors would reduce neovascularization and inflammation [43, 63] and provide an enabling environment to promote the proliferation and differentiation of the resident stem cells in the tissues [73, 74]. Although the anti-angiogenic and the anti-inflammatory capacity of hAT-MSCs have been reported [22–24], this is the first time that the capability of these cells to recover the corneal and limbal phenotypes has been demonstrated in *in vivo* models.

CONCLUSION

Overall, our results indicate that hAT-MSCs transplanted to the ocular surface are well tolerated, migrate to inflamed tissues, reduce inflammation, restrain the evolution of neovascularization and corneal opacification, and partially restore limbal and corneal epithelial phenotypes. This suggests that hAT-MSC transplantation could be a novel therapy to treat patients suffering from ocular surface failure due to LSCD. hAT-MSCs represent an efficient source of stem cells with no availability limitations, and which have immunomodulatory and regenerative properties that may provide therapeutic benefits and reduce health care expenses.

ACKNOWLEDGMENTS

We thank M. J. Villanueva (Europa Clinic, Valladolid, Spain) and the Tissue Establishment (San Francisco Clinic, León, Spain) for their support in providing human liposuction and amniotic membrane, I. Fernández (IOBA, University of Valladolid, Spain) for statistical assistance, J. C. López (IOBA-Ocular Pathology Laboratory, University of Valladolid, Spain) for his guidance, and B. Bromberg (Certified Editor in Life

Sciences of Xenofile Editing, www.xenofileediting.com) for his assistance in the final editing and preparation of this manuscript. This work was supported by Instituto de Salud Carlos III, CIBER-BBN, Spain (CB06/01/003 MINECO/FEDER, EU); Regional Center for Regenerative Medicine and Cell Therapy, Castilla y León, Spain; Ministry of Science and Innovation, Spain (SAF2010–14900); Ministry of Economy and Competitiveness and European Regional Development Fund, Spain (SAF2015–63594-R MINECO/FEDER, EU); and scholarships by the Junta de Castilla y León and the European Social Fund (to S.G., M.L.-P., and M.P.-C.). This work was presented in part at the 2014 and 2015 annual meetings of the Association for Research in Vision and Ophthalmology (ARVO): Invest Ophthalmol Vis Sci 2014; 55:ARVO E-abstract 5162. Invest Ophthalmol Vis Sci 2015; 56:ARVO E-abstract 3474. Invest Ophthalmol Vis Sci 2015; 56:ARVO E-abstract 5638. E.R. is currently affiliated with the Hospital Universitario Santa Cristina, Instituto de Investigación Sanitaria Princesa (IIS-P), Madrid, Spain; A.d.I.M. is currently affiliated with the Department of Physiology and Membrane Biology, University of California, Davis, CA.

AUTHOR CONTRIBUTIONS

S.G.: conception and design, collection and/or assembly of data, data analysis and interpretation, manuscript writing, approved the final manuscript; J.M.H.: conception and design, performance of surgical procedures, data interpretation, approved the final manuscript; M.L.-P., A.d.I.M., and M.P.-C.: collection and/or assembly of data, approved the final manuscript; E.R.: collection and/or assembly of data, technical support, approved the final manuscript; M.C. and T.N.-M.: conception and design, data analysis and interpretation, manuscript writing, financial support, approved the final manuscript. M.C. and T.N.-M. are senior co-authors.

DISCLOSURE OF POTENTIAL CONFLICTS OF INTEREST

The authors indicated no potential conflicts of interest.

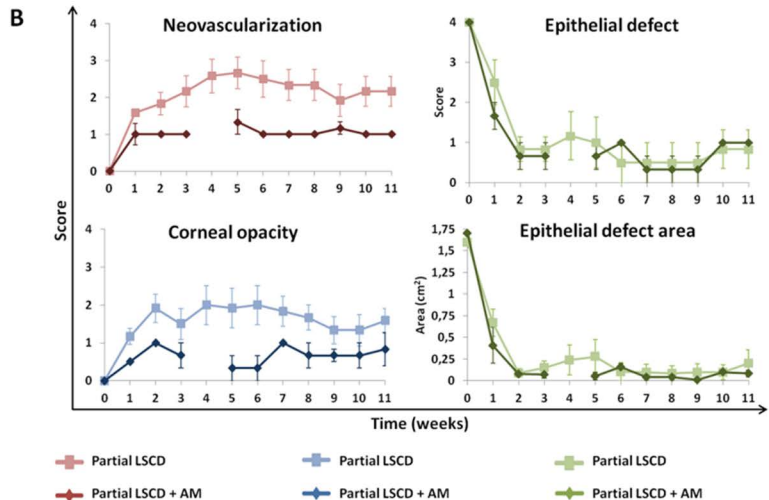
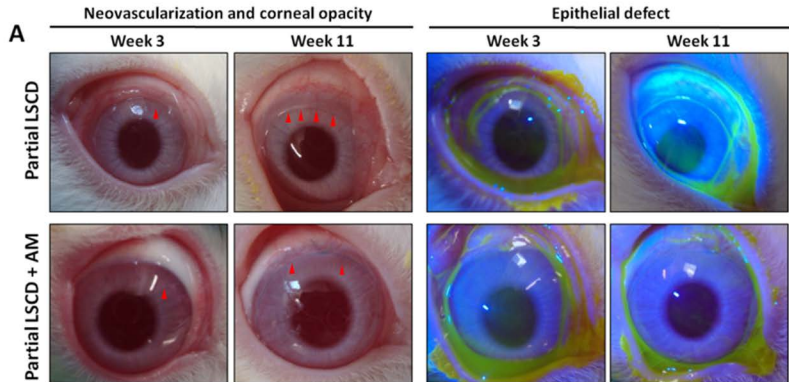
REFERENCES

- 1** Cotsarelis G, Cheng SZ, Dong G et al. Existence of slow-cycling limbal epithelial basal cells that can be preferentially stimulated to proliferate: Implications on epithelial stem cells. *Cell* 1989;57:201–209.
- 2** Li W, Hayashida Y, Chen YT et al. Niche regulation of corneal epithelial stem cells at the limbus. *Cell Res* 2007;17:26–36.
- 3** Schlotzer-Schreiber U, Kruse FE. Identification and characterization of limbal stem cells. *Exp Eye Res* 2005;81:247–264.
- 4** Dua HS, Saini JS, Azuara-Blanco A et al. Limbal stem cell deficiency: Concept, aetiology, clinical presentation, diagnosis and management. *Indian J Ophthalmol* 2000;48:83–92.
- 5** Sejpal K, Bakhtiari P, Deng SX. Presentation, diagnosis and management of limbal stem cell deficiency. *Middle East Afr J Ophthalmol* 2013;20:5–10.
- 6** Shortt AJ, Secker GA, Rajan MS et al. Ex vivo expansion and transplantation of limbal epithelial stem cells. *Ophthalmology* 2008;115:1989–1997.
- 7** Rama P, Matuska S, Paganoni G et al. Limbal stem-cell therapy and long-term corneal regeneration. *N Engl J Med* 2010;363:147–155.
- 8** Ramirez BE, Sanchez A, Herreras JM et al. Stem cell therapy for corneal epithelium regeneration following good manufacturing and clinical procedures. *Biomed Res Int* 2015;2015:408495.
- 9** Joe AW, Gregory-Evans K. Mesenchymal stem cells and potential applications in treating ocular disease. *Curr Eye Res* 2010;35:941–952.
- 10** Ren G, Chen X, Dong F et al. Concise review: Mesenchymal stem cells and translational medicine: Emerging issues. *STEM CELLS TRANS MED* 2012;1:51–58.
- 11** Yao L, Bai H. Review: Mesenchymal stem cells and corneal reconstruction. *Mol Vis* 2013;19:2237–2243.
- 12** Zhang L, Coulson-Thomas VJ, Ferreira TG et al. Mesenchymal stem cells for treating ocular surface diseases. *BMC Ophthalmol* 2015;15 Suppl 1:155.
- 13** Jackson L, Jones DR, Scotting P et al. Adult mesenchymal stem cells: Differentiation potential and therapeutic applications. *J Postgrad Med* 2007;53:121–127.
- 14** Aggarwal S, Pittenger MF. Human mesenchymal stem cells modulate allogeneic immune cell responses. *Blood* 2005;105:1815–1822.
- 15** Holan V, Javorkova E. Mesenchymal stem cells, nanofiber scaffolds and ocular surface reconstruction. *Stem Cell Rev* 2013;9:609–619.
- 16** Harkin DG, Foyn L, Bray LJ et al. Concise reviews: Can mesenchymal stromal cells differentiate into corneal cells? A systematic review of published data. *STEM CELLS* 2015;33:785–791.
- 17** Strioga M, Viswanathan S, Darinskas A et al. Same or not the same? Comparison of adipose tissue-derived versus bone marrow-derived mesenchymal stem and stromal cells. *Stem Cells Dev* 2012;21:2724–2752.
- 18** Nieto-Miguel T, Galindo S, Reinoso R et al. In vitro simulation of corneal epithelium microenvironment induces a corneal epithelial-like cell phenotype from human adipose tissue mesenchymal stem cells. *Curr Eye Res* 2013;38:933–944.
- 19** Martinez-Conesa EM, Espel E, Reina M et al. Characterization of ocular surface epithelial and progenitor cell markers in human adipose stromal cells derived from lipoaspirates. *Invest Ophthalmol Vis Sci* 2011;53:513–520.
- 20** Lin HF, Lai YC, Tai CF et al. Effects of cultured human adipose-derived stem cells transplantation on rabbit cornea regeneration after alkaline chemical burn. *Kaohsiung J Med Sci* 2013;29:14–18.
- 21** Lin KJ, Loi MX, Lien GS et al. Topical administration of orbital fat-derived stem cells promotes corneal tissue regeneration. *Stem Cell Res Ther* 2013;4:72.
- 22** Zeppieri M, Salvetat ML, Beltrami AP et al. Human adipose-derived stem cells for the treatment of chemically burned rat cornea: Preliminary results. *Curr Eye Res* 2013;38:451–463.
- 23** Almaliotis D, Koliakos G, Papakonstantinou E et al. Mesenchymal stem cells improve healing of the cornea after alkali injury. *Graefes Arch Clin Exp Ophthalmol* 2015; 253:1121–1135.
- 24** Espardar L, Caldwell D, Watson R et al. Application of adipose-derived stem cells on scleral contact lens carrier in an animal model of severe acute alkaline burn. *Eye Contact Lens* 2014;40:243–247.
- 25** Holan V, Trosan P, Cejka C et al. A comparative study of the therapeutic potential of mesenchymal stem cells and limbal epithelial stem cells for ocular surface reconstruction. *Stem Cells Trans Med* 2015;4:1052–1063.
- 26** Agorogiannis GI, Alexaki VI, Castana O et al. Topical application of autologous adipose-derived mesenchymal stem cells (MSCs) for persistent sterile corneal epithelial defect. *Graefes Arch Clin Exp Ophthalmol* 2011;250:455–457.
- 27** Zuk PA, Zhu M, Mizuno H et al. Multilineage cells from human adipose tissue: Implications for cell-based therapies. *Tissue Eng* 2001;7:211–228.
- 28** Dominici M, Le BK, Mueller I et al. Minimal criteria for defining multipotent mesenchymal stromal cells. The International Society for Cellular Therapy position statement. *Cytotherapy* 2006;8:315–317.
- 29** Tseng SC. Amniotic membrane transplantation for ocular surface reconstruction. *Biosci Rep* 2001;21:481–489.
- 30** Wan P, Wang X, Ma P et al. Cell delivery with fixed amniotic membrane reconstructs corneal epithelium in rabbits with limbal stem cell deficiency. *Invest Ophthalmol Vis Sci* 2011;52:724–730.
- 31** Efron N. Grading scales for contact lens complications. *Ophthalmic Physiol Opt* 1998; 18:182–186.
- 32** Kasper M, Moll R, Stosiek P et al. Patterns of cytokeratin and vimentin expression in the human eye. *Histochemistry* 1988;89:369–377.
- 33** Chen Z, de Paiva CS, Luo L et al. Characterization of putative stem cell phenotype in human limbal epithelia. *STEM CELLS* 2004;22:355–366.

- 34** Yoshida S, Shimmura S, Kawakita T et al. Cytokeratin 15 can be used to identify the limbal phenotype in normal and diseased ocular surfaces. *Invest Ophthalmol Vis Sci* 2006;47:4780–4786.
- 35** Pellegrini G, Dellambra E, Golisano O et al. P63 identifies keratinocyte stem cells. *Proc Natl Acad Sci USA* 2001;98:3156–3161.
- 36** Krenzer KL, Freddo TF. Cytokeratin expression in normal human bulbar conjunctiva obtained by impression cytology. *Invest Ophthalmol Vis Sci* 1997;38:142–152.
- 37** Hayashi S, Osawa T, Tohyama K. Comparative observations on corneas, with special reference to Bowman's layer and Descemet's membrane in mammals and amphibians. *J Morphol* 2002;254:247–258.
- 38** Higa K, Shimmura S, Kato N et al. Proliferation and differentiation of transplantable rabbit epithelial sheets engineered with or without an amniotic membrane carrier. *Invest Ophthalmol Vis Sci* 2007;48:597–604.
- 39** Omoto M, Miyashita H, Shimmura S et al. The use of human mesenchymal stem cell-derived feeder cells for the cultivation of transplantable epithelial sheets. *Invest Ophthalmol Vis Sci* 2009;50:2109–2115.
- 40** Reinshagen H, Uw-Haedrich C, Sorg RV et al. Corneal surface reconstruction using adult mesenchymal stem cells in experimental limbal stem cell deficiency in rabbits. *Acta Ophthalmol* 2009;89:741–748.
- 41** Chen JJ, Tseng SC. Corneal epithelial wound healing in partial limbal deficiency. *Invest Ophthalmol Vis Sci* 1990;31:1301–1314.
- 42** Hayashida Y, Nishida K, Yamato M et al. Ocular surface reconstruction using autologous rabbit oral mucosal epithelial sheets fabricated ex vivo on a temperature-responsive culture surface. *Invest Ophthalmol Vis Sci* 2005;46:1632–1639.
- 43** Yao L, Li ZR, Su WR et al. Role of mesenchymal stem cells on cornea wound healing induced by acute alkali burn. *PLoS One* 2012;7:e30842.
- 44** Xu B, Fan TJ, Zhao J et al. Transplantation of tissue-engineered human corneal epithelium in limbal stem cell deficiency rabbit models. *Int J Ophthalmol* 2012;5:424–429.
- 45** Figueroa-Ortiz LC, Martin Rodriguez O, Garcia-Ben A et al. Neovascular growth in an experimental alkali corneal burn model. *Arch Soc Esp Oftalmol* 2014;89:303–307.
- 46** Zhang W, Yang W, Liu X et al. Rapidly constructed scaffold-free embryonic stem cell sheets for ocular surface reconstruction. *Scanning* 2014;36:286–292.
- 47** Ma Y, Xu Y, Xiao Z et al. Reconstruction of chemically burned rat corneal surface by bone marrow-derived human mesenchymal stem cells. *STEM CELLS* 2006;24:315–321.
- 48** Anderson DF, Ellies P, Pires RT et al. Amniotic membrane transplantation for partial limbal stem cell deficiency. *Br J Ophthalmol* 2001;85:567–575.
- 49** Dua HS, Gomes JA, King AJ et al. The amniotic membrane in ophthalmology. *Surv Ophthalmol* 2004;49:51–77.
- 50** Tseng SC, Prabhasawat P, Barton K et al. Amniotic membrane transplantation with or without limbal allografts for corneal surface reconstruction in patients with limbal stem cell deficiency. *Arch Ophthalmol* 1998;116:431–441.
- 51** Rohaina CM, Then KY, Ng AM et al. Reconstruction of limbal stem cell deficient corneal surface with induced human bone marrow mesenchymal stem cells on amniotic membrane. *Transl Res* 2014;163:200–210.
- 52** Rehman J, Traktuev D, Li J et al. Secretion of angiogenic and antiapoptotic factors by human adipose stromal cells. *Circulation* 2004;109:1292–1298.
- 53** Lee RH, Yu JM, Foskett AM et al. TSG-6 as a biomarker to predict efficacy of human mesenchymal stem/progenitor cells (hMSCs) in modulating sterile inflammation in vivo. *Proc Natl Acad Sci USA* 2014;111:16766–16771.
- 54** Pinarli FA, Okten G, Beden U et al. Keratinocyte growth factor-2 and autologous serum potentiate the regenerative effect of mesenchymal stem cells in cornea damage in rats. *Int J Ophthalmol* 2014;7:211–219.
- 55** Acar U, Pinarli FA, Acar DE et al. Effect of allogeneic limbal mesenchymal stem cell therapy in corneal healing: Role of administration route. *Ophthalmic Res* 2015;53:82–89.
- 56** Ke Y, Wu Y, Cui X et al. Polysaccharide hydrogel combined with mesenchymal stem cells promotes the healing of corneal alkali burn in rats. *PLoS One* 2015;10:e0119725.
- 57** Li F, Zhao SZ. Mesenchymal stem cells: Potential role in corneal wound repair and transplantation. *World J Stem Cells* 2014;6:296–304.
- 58** Ahmed SK, Soliman AA, Omar SM et al. Bone marrow mesenchymal stem cell transplantation in a rabbit corneal alkali burn model (a histological and immune histo-chemical study). *Int J Stem Cells* 2015;8:69–78.
- 59** Roddy GW, Oh JY, Lee RH et al. Action at a distance: Systemically administered adult stem/progenitor cells (MSCs) reduce inflammatory damage to the cornea without engraftment and primarily by secretion of TNF-alpha stimulated gene/protein 6. *STEM CELLS* 2011;29:1572–1579.
- 60** Oh JY, Roddy GW, Choi H et al. Anti-inflammatory protein TSG-6 reduces inflammatory damage to the cornea following chemical and mechanical injury. *Proc Natl Acad Sci USA* 2010;107:16875–16880.
- 61** Fatima A, Iftekhar G, Sangwan VS et al. Ocular surface changes in limbal stem cell deficiency caused by chemical injury: A histologic study of excised pannus from recipients of cultured corneal epithelium. *Eye (Lond)* 2008;22:1161–1167.
- 62** Wei ZG, Wu RL, Lavker RM et al. In vitro growth and differentiation of rabbit bulbar, fornix, and palpebral conjunctival epithelia. Implications on conjunctival epithelial trans-differentiation and stem cells. *Invest Ophthalmol Vis Sci* 1993;34:1814–1828.
- 63** Oh JY, Kim MK, Shin MS et al. The anti-inflammatory and anti-angiogenic role of mesenchymal stem cells in corneal wound healing following chemical injury. *STEM CELLS* 2008;26:1047–1055.
- 64** Sohni A Verfaillie CM. Mesenchymal stem cells migration homing and tracking. *Stem Cells Int* 2013;2013:130763.
- 65** Dotan I, Werner L, Vigodman S et al. CXCL12 is a constitutive and inflammatory chemokine in the intestinal immune system. *Inflamm Bowel Dis* 2010;16:583–592.
- 66** Nieto-Miguel T, Calonge M, de la Mata A et al. A comparison of stem cell-related gene expression in the progenitor-rich limbal epithelium and the differentiating central corneal epithelium. *Mol Vis* 2011;17:2102–2117.
- 67** Xie HT, Chen SY, Li GG et al. Limbal epithelial stem/progenitor cells attract stromal niche cells by SDF-1/CXCR4 signaling to prevent differentiation. *STEM CELLS* 2011;29:1874–1885.
- 68** Kameishi S, Sugiyama H, Yamato M et al. Remodeling of epithelial cells and basement membranes in a corneal deficiency model with long-term follow-up. *Lab Invest* 2015;95:168–179.
- 69** Ng GY, Yeh LK, Zhang Y et al. Role of SH2-containing tyrosine phosphatase Shp2 in mouse corneal epithelial stratification. *Invest Ophthalmol Vis Sci* 2013;54:7933–7942.
- 70** Lin Z, He H, Zhou T et al. A mouse model of limbal stem cell deficiency induced by topical medication with the preservative benzalkonium chloride. *Invest Ophthalmol Vis Sci* 2013;54:6314–6325.
- 71** Lan Y, Kodati S, Lee HS et al. Kinetics and function of mesenchymal stem cells in corneal injury. *Invest Ophthalmol Vis Sci* 2012;53:3638–3644.
- 72** Gu S, Xing C, Han J et al. Differentiation of rabbit bone marrow mesenchymal stem cells into corneal epithelial cells in vivo and ex vivo. *Mol Vis* 2009;15:99–107.
- 73** Oh JY, Ko JH, Kim MK et al. Effects of mesenchymal stem/stromal cells on cultures of corneal epithelial progenitor cells with ethanol injury. *Invest Ophthalmol Vis Sci* 2014;55:7628–7635.
- 74** Hu N, Zhang YY, Gu HW et al. Effects of bone marrow mesenchymal stem cells on cell proliferation and growth factor expression of limbal epithelial cells in vitro. *Ophthalmic Res* 2012;48:82–88.



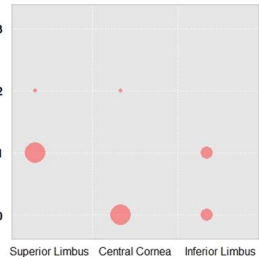
See www.StemCells.com for supporting information available online.



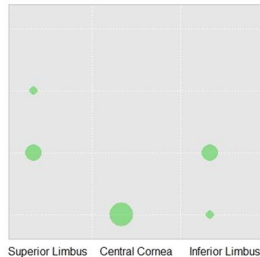
Partial LSCD model

• Inflammatory cells ■ hAT-MSCs

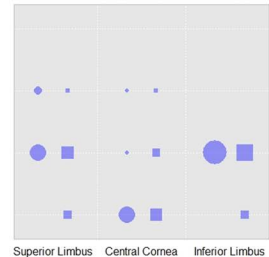
Presence of cells



Partial LSCD



Partial LSCD + AM



Partial LSCD + AM + hAT-MSCs

Total LSCD model

• Inflammatory cells ■ hAT-MSCs

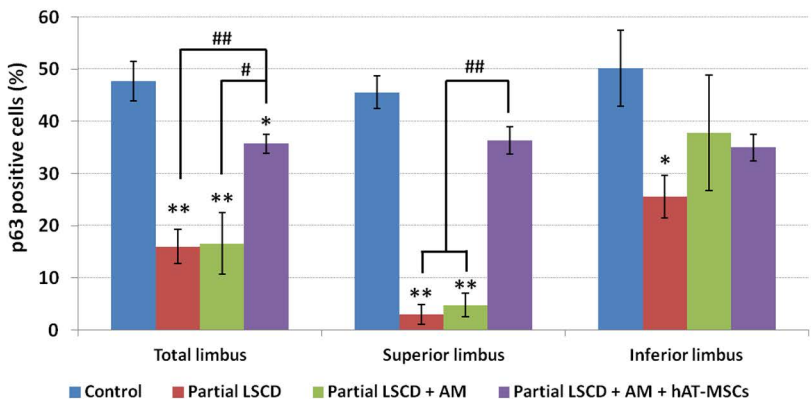


Total LSCD

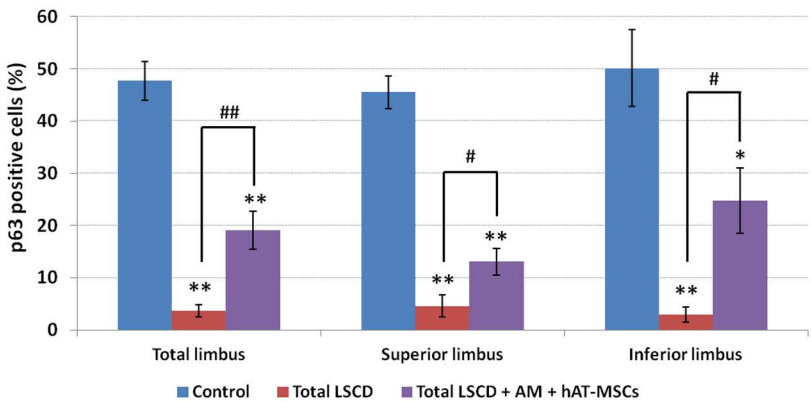


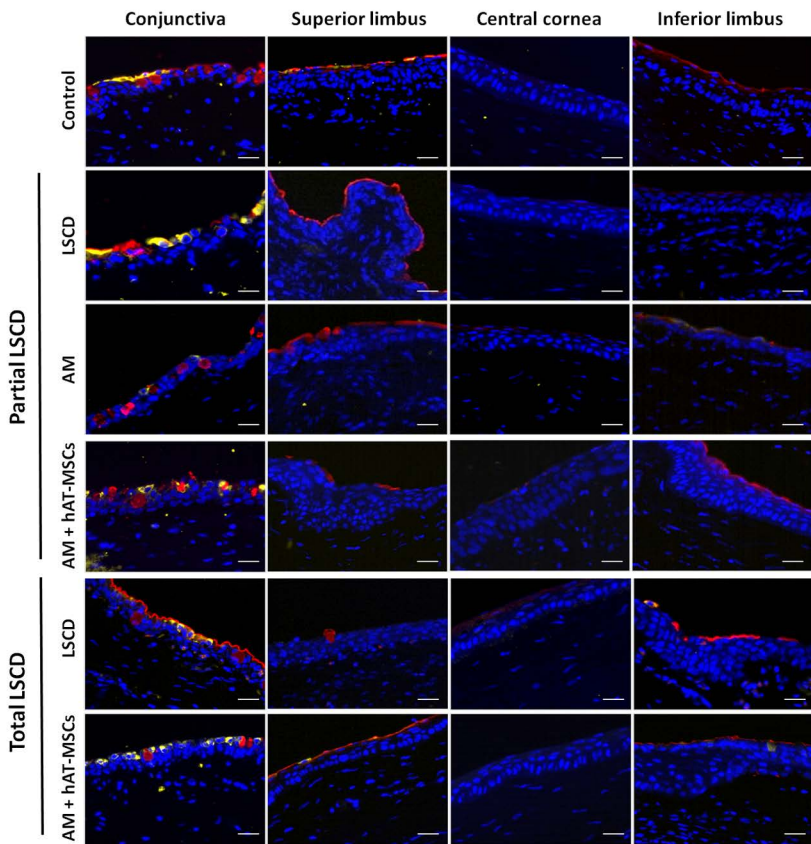
Total LSCD + AM + hAT-MSCs

Partial LSCD model



Total LSCD model





SUPPLEMENTAL TABLES

Table S1. Treatment groups.

Group (n)	LSCD	Treatment
0 (6)	None	None
1 (6)	Partial	None
2 (3)	Partial	AM
3 (6)	Partial	AM + hAT-MSCs
4 (6)	Total	None
5 (5)	Total	AM + hAT-MSCs

n, number of animals; LSCD, limbal stem cell deficiency; AM, amniotic membrane; hAT-MSCs, human adipose tissue-derived mesenchymal stem cells. "Partial" refers to the LSCD model that covered 180° and included the superior and temporal limbus. "Total" refers to the LSCD that included the entire limbus.

Table S2. Criteria for ocular surface evaluation.

Score	Neovascularization	Corneal opacity	Epithelial defect	Conjunctival invasion
0	None	None	None	None
1	Area ≤ 1/4	Mild	Area ≤ 1/4	Area ≤ 1/4
2	1/4 < area ≤ 1/2	Moderate	1/4 < area ≤ 1/2	1/4 < area ≤ 1/2
3	1/2 < area ≤ 3/4	Severe, pupil seen faintly	1/2 < area ≤ 3/4	1/2 < area ≤ 3/4
4	Area > 3/4	Severe, pupil not visible	Area > 3/4	Area > 3/4

Table S3. Primary and secondary antibodies used in immunofluorescence experiments.

Antibody	Specificity/Type	Clone	Source	Dilution
Anti-BrdU-DyLight650	hAT-MSCs marked with BrdU	Polyclonal	Novus Biologicals	1:100
Anti-CK3	Corneal epithelial cells	AE5	Mp Biomedical	1:50
Anti-CK7	Conjunctival cells	OV-TL 12/30	Vector Laboratories	1:50
Anti-CK15	Limbal epithelial stem cells	LHK15	Merck	1:50
Anti-E-cadherin	Corneal epithelial cells	36	BD Biosciences	1:100
Anti-p63	Limbal epithelial stem cells	4A4	Santa Cruz	1:50
Anti-mouse (PECy5)	Secondary antibody	Polyclonal	Santa Cruz	1:100

Novus Biologicals (Littleton, CO, USA), Mp Biomedical (Illkirch, France), Vector Laboratories (Burlingame, CA, USA), Merck (Darmstadt, Germany), BD Biosciences (San Jose, CA, USA), Santa Cruz (Dallas, TX, USA).

Table S4. CK3, E-cadherin, CK15, p63, and CK7 expression in the partial and total limbal stem cell deficiency (LSCD) models.

	Corneal epithelial cell markers						Limbal stem cell markers						Conjunctival cell marker			
	CK3			E-cadherin			CK15			p63			CK7			
	SL	CC	IL	SL	CC	IL	SL	CC	IL	SL	CC	IL	CJ	SL	CC	IL
Control	+	+++	+	-	+++	-	+++	-	+++	+++	-	+++	+++	+	-	+
Partial LSCD	++	+++	++	-	+++	-	-	-	+++	-	-	+++	+++	+	-	+
AM	+	+	+	-	+++	-	-	-	+++	-	-	+++	+++	+	-	+
AM + hAT-MSCs	+	+++	+	+	+++	-	+++	-	+++	++	-	+++	+++	+	-	+
Total LSCD	-	-	-	-	+	-	-	-	-	-	-	-	+++	+	-	+
AM + hAT-MSCs	++	+	++	++	+++	++	+++	++	+++	-	-	++	+++	+	-	+

Subjective evaluation: - absence; + mild expression; ++ moderate expression; +++ high expression. AM: amniotic membrane, hAT-MSCs: human adipose tissue-derived mesenchymal stem cells, SL: superior limbus, CC: central cornea, IL: inferior limbus, CJ: conjunctiva.

Supplemental Figure Legends

Figure S1. Ocular surface evaluation in the partial limbal stem cell deficiency (LSCD) model without treatment or transplanted with amniotic membrane (AM).

Neovascularization (red arrowheads) and corneal opacification developed during the first weeks after injury. Epithelial defects partially recovered during the first 2 weeks. There were no differences in the clinical signs of the untreated partial LSCD model and the partial LSCD model transplanted with AM. Data for week 0 was acquired immediately after the partial limbectomy. Data for Week 3 was acquired immediately before transplantation. Representative images from animals of each group.

Figure S2. Inflammatory cells and hAT-MSCs in the ocular surface tissues of partial and total limbal stem cell deficiency (LSCD) models.

Subjective evaluation: 0, absence; 1, low amount; 2, moderate amount; 3, high amount. The size of the points is proportional to the relative frequency of animals that belong to each category of the scale. There were no differences in the presence of inflammatory cells among the three groups of the partial LSCD model. In the total LSCD model, hAT-MSC transplanted eyes had fewer inflammatory cells in comparison with the non-transplanted group. The hAT-MSCs were located in the inflamed areas of the superior and inferior limbal stroma 8 weeks after transplantation in both partial and total LSCD models. The hAT-MSCs were located in the central cornea of the animals with inflammation in this area. The correlation between the amount of hAT-MSCs transplanted and the level of inflammation

in the cornea was significant ($r=0.810$; $p=0.003$). AM, amniotic membrane; hAT-MSCs, human adipose tissue-derived mesenchymal stem cells.

Figure S3. p63 expression in partial and total limbal stem cell deficiency (LSCD) models. In the limbal epithelium of the partial LSCD model, the percentage of p63-positive cells was significantly lower than in the control healthy group. Very similar results were observed in the limbal epithelium of the animals transplanted with cell-free AM. Thus there were significant differences with the healthy control group in the total limbus and in the superior limbus, but not in the inferior limbus or in comparison with the untreated group. The expression of p63-positive cells was significantly lower in the hAT-MSC transplanted group in comparison with the healthy control group. However, the expression of p63 was partially restored in the hAT-MSC transplanted group, especially in the superior limbus, where there were significant differences in comparison with the untreated group and with the AM transplanted group. In the total LSCD model, the percentage of p63-positive cells was significantly lower in the untreated group than in the healthy control group. The hAT-MSC transplanted group had a lower percentage of cells that expressed p63 than the healthy control group. However, the percentage of p63-positive cells was partially restored in the hAT-MSC transplanted group, especially in the inferior limbus, in comparison with the untreated group. * $p\leq0.05$ and ** $p\leq0.01$ in comparison with the healthy control group. # $p\leq0.05$ and ## $p\leq0.01$ in comparison with the hAT-MSC transplanted group.

Figure S4. Immunofluorescence microscopy of CK7 expression, a conjunctival cell marker, in the ocular surface of the partial and total limbal stem cell deficiency (LSCD) models at the end of the follow-up period. In healthy control eyes, expression of CK7 (yellow) was present in the conjunctival epithelium and in some cells of the limbal epithelium. There were no differences in the CK7 expression among the different groups within the partial and total LSCD models. Goblet cells mucins in the conjunctiva and in the limbus of the healthy eyes were stained by lectin. Additionally, there was a diffuse staining on the surface of conjunctival and limbal epithelium, indicating the presence of secreted mucins. Except for the central cornea of the total LSCD model, there were no differences in lectin staining among the partial or total LCSD groups. In 2 of the 6 animals with untreated total LSCD, goblet cells were present in the central cornea. However, just 1 animal with total LSCD with AM + hAT-MSC transplantation had goblet cells in the central cornea. Nuclei, blue. Representative images from each group.
Scale bar: 100 μ m.